

NASA Contractor Report 172232



CALCULATION OF WING RESPONSE TO GUSTS AND BLAST WAVES WITH VORTEX LIFT EFFECT

(NACA-CR-172232) CALCULATION OF WING
RESPONSE TO GUSTS AND BLAST WAVES WITH
VORTEX LIFT EFFECT Contractor Report, Jun.
1981 - Dec. 1982 (Kansas Univ.) 66 p
HC A04/MF A01

N83-35997

Unclas
CSCI 01A G3/02 42224

Der-Chang Chao and C. Edward Lan

THE UNIVERSITY OF KANSAS CENTER FOR RESEARCH, INC.
Flight Research Laboratory
Lawrence, Kansas 66045

Grant NAG1-75
October 1983

NASA
National Aeronautics and
Space Administration
Langley Research Center
Hampton, Virginia 23665

TABLE OF CONTENTS

| | <u>Page</u> |
|--|-------------|
| 1. INTRODUCTION | 1 |
| 2. MATHEMATICAL FORMULATION | 4 |
| 2.1 Two-Dimensional Gust Penetration | 4 |
| 2.2 Three-Dimensional Gust Penetration | 8 |
| 2.3 Padé Approximant | 10 |
| 2.4 Least Square Technique | 11 |
| 2.5 Indicial Lift Function | 12 |
| 2.6 Nuclear Blast Response | 12 |
| 3. NUMERICAL RESULTS AND DISCUSSIONS | 15 |
| 3.1 Gust Penetration | 15 |
| 3.1.1 Sinusoidal gust problem | 15 |
| 3.1.2 Padé approximant | 17 |
| 3.1.3 Indicial lift function | 18 |
| 3.1 Nuclear Blast Response | 19 |
| 4. CONCLUSIONS AND RECOMMENDATIONS | 22 |
| 5. REFERENCES | 24 |

LIST OF ILLUSTRATIONS

| <u>Figure</u> | <u>Page</u> |
|---|-------------|
| 1. Thin airfoil passing through a region of harmonic gusts with vertical gust velocity distribution $\bar{w}_g(x,t)$ | 30 |
| 2. Generalized oscillatory lift for a 75° delta wing due to harmonic gusts with $\bar{w}_g = 1$ at $M = 0.4$ | 31 |
| 3. Generalized oscillatory pitching moment for a 75° delta wing due to harmonic gusts with $\bar{w}_g = 1$ at $M = 0.4$; pitching axis at root midchord point | 32 |
| 4. Incremental lift for a rectangular wing of $AR = 6$ due to sinusoidal gusts for $\alpha = 0^\circ$ with $\bar{w}_g = 0.0314$ and reference point at root quarter chord point | 33 |
| 5. Incremental lift for a delta wing of $AR = 1$ in sinusoidal gusts for $\alpha = 0$ and 12 degrees with $\bar{w}_g = 0.0314$ and reference point at root 2/3rd chord point | 34 |
| 6. Incremental lift for a delta wing of $AR = 1$ in sinusoidal gusts for $\alpha = 0^\circ$ with $\bar{w}_g = 0.0314$ and reference point at root 2/3rd chord point | 35 |
| 7. Variations of phase angle due to changes of angle of attack and reference points for a delta wing of $AR = 1$ in sinusoidal gusts | 36 |
| 8. Oscillatory lift for a thin airfoil due to harmonic gusts with $\bar{w}_g = 1$ at $M = 0$ | 37 |
| 9. Oscillatory lift for a thin airfoil due to harmonic gusts with $\bar{w}_g = 1$ at $M = 0.5$ | 38 |
| 10. Oscillatory lift for a thin airfoil due to harmonic gusts with $\bar{w}_g = 1$ at $M = 0.7$ | 39 |
| 11. Oscillatory lift for a delta wing of $AR = 1.2$ in sinusoidal gusts for $\alpha = 0^\circ$ with $\bar{w}_g = 0.261$ at $M = 0.16$ | 40 |
| 12. Oscillatory lift for a delta wing of $AR = 1.2$ in sinusoidal gusts for $\alpha = 14.6^\circ$ with $\bar{w}_g = -0.261$ at $M = 0.16$ | 41 |

LIST OF ILLUSTRATIONS (CONT'D)

| <u>Figure</u> | <u>Page</u> |
|---|-------------|
| 13. Indicial lift function from a sharp-edged gust of a thin airfoil at $M=0$ | 42 |
| 14. Indicial lift function from a sharp-edged gust of a thin airfoil at $M=0.5$ | 43 |
| 15. Indicial lift function from a sharp-edged gust of a thin airfoil at $M=0.7$ | 44 |
| 16. Indicial lift function for a thin airfoil entering into a sharp-edged gust in subsonic compressible flow | 45 |
| 17. General configuration and transducer positions of a test wing and definitions of local span and distance parameter penetrated into vertical gusts in reference 11 | 46 |
| 18. Trend of indicial lift function from vertical gusts of a delta wing of $AR = 1.2$ at $M = 0.16$ | 48 |
| 19. Indicial lift function for a delta wing of $AR = 1.2$ entering into vertical gusts at $M = 0.16$ | 51 |
| 20. Thin wing intercepted by a blast wave moving with sonic speed . | 52 |
| 21. General configuration of a test model used for nuclear blast response (taken from reference 17) | 53 |
| 22. Simplified wing planform used by the present theory for nuclear blast response analysis | 54 |
| 23. Pressure variation of the test wing due to nuclear blast waves with $\theta = 20^\circ$ for $\alpha = 3.2^\circ$ at $M = 0.76$ (reproduced from Ref. 17) . | 55 |
| 24. Impulse lift function of the test wing due to nuclear blast waves with $\theta = 20^\circ$ for $\alpha = 3.2^\circ$ at $M = 0.76$ | 56 |

LIST OF TABLES

| <u>Table</u> | <u>Page</u> |
|--|-------------|
| 1. Oscillatory lift on a thin airfoil due to a sinusoidal gust at $M=0$ | 27 |
| 2. Oscillatory lift on a thin airfoil due to a sinusoidal gust at $k=2.0$ | 28 |

NOMENCLATURE

| | |
|------------------|--|
| A_i | = coefficients of Padé approximant |
| AR | = wing aspect ratio |
| B_i | = coefficients of partial fraction of Padé approximant |
| b_n | = local span at the section containing the transducer as shown in Fig. 17(b) |
| \bar{c} | = reference chord |
| c^* | = semichord length of the airfoil |
| $C(k)$ | = Theodorsen function |
| $C_C(k)$ | = generalized Theodorsen function |
| C_l | = two-dimensional oscillatory lift coefficient |
| C_{l_0} | = two-dimensional steady state lift coefficient |
| C_m | = oscillatory pitching moment due to sinusoidal gusts |
| F | = Fourier transform |
| $F(k)$ | = $C(k)[J_0(k) - iJ_1(k)] + iJ_1(k)$ |
| $h(s)$ | = impulse lift function due to nuclear blast |
| $J_0(k), J_1(k)$ | = Bessel functions of the first kind |
| k | = $\omega \bar{c} / U$, reduced frequency |
| k' | = $k / 0.61$, effective reduced frequency |
| \mathcal{L} | = Laplace transform |
| L | = oscillatory lift distribution |
| $L'(k)$ | = in-phase component of oscillatory lift coefficient |
| $L''(k)$ | = out-of-phase component of oscillatory lift coefficient |
| M | = freestream Mach number |
| r | = ik , Laplace transform variable |
| s | = Ut/c^* or Ut/\bar{c} , non-dimensional distance parameter |
| S | = reference wing area |

| | |
|----------------|--|
| t | = time coordinate |
| $T(k)$ | = $L'(k) + iL''(k)$, oscillatory lift coefficient due to sinusoidal gusts |
| U | = freestream velocity |
| $V(k) + iW(k)$ | = $1 - T(k)$, [see Eq. (30)] |
| w_a | = vertical velocity component of the vortex sheet simulating the airfoil in gust field |
| w_a^* | = amplitude of w_a |
| \bar{w}_a | = w_a^* / U |
| w_g | = vertical velocity component of gust |
| w_g^* | = amplitude of vertical velocity component of gust |
| \bar{w}_g | = w_g^* / U |
| w_0 | = vertical velocity component of a sharp-edged gust |
| \bar{x} | = x/c^* or x/\bar{c} , non-dimensional x-coordinate |
| x_{le} | = x-coordinate of wing leading edge |
| x_R | = reference point for gust phase |
| x_n | = distance penetrated into a step gust, [see Fig. 17(b)] |
| x, z | = Cartesian coordinate system [see Fig. 1] |
| α | = angle of attack |
| β | = $\sqrt{1-M^2}$ |
| β_i | = root of the polynomial in the denominator of Padé approximant, which is always real |
| $\delta(t)$ | = delta function |
| θ | = blast intercept angle (see Fig. 20) |
| ρ | = freestream density |
| ϕ | = phase difference (in degrees) of oscillatory lift |
| $\psi(s)$ | = indicial lift due to step gusts |
| ω | = radian frequency associated with the gust wavelength |

1. INTRODUCTION

Estimation of the response of an aircraft due to atmospheric gusts has been the subject of numerous investigations from the viewpoint of producing useful data on the induced aerodynamic forces for the design of active control systems for gust alleviation.

In theoretical analyses, the change of lift and moment on a wing passing through a sharp-edged gust was first calculated for incompressible two-dimensional flow by Kármán and Sears with simple mathematical formulae (Ref. 1). Miles (Ref. 2) extended the calculations to a travelling gust field, i.e., sharp-edged gust moving either downstream or upstream relative to the airfoil. Drischler and Diederich (Ref. 3) presented results for a wide range of wings in both incompressible and compressible flows. Meanwhile, the response of an airfoil entering a harmonic gust field was first introduced by Sears (Ref. 4). Murrow, et al. (Ref. 5) provided many numerical results of lift and moment for finite wings moving through a harmonic gust. Giesing, et al. (Ref. 6) also furnished some good suggestions in computing the oscillatory lift and moment. One notable method, called the Doublet Lattice Method (DLM) which was originally developed by Albano and Rodden (Ref. 7), was later improved to become a very useful tool in unsteady aerodynamics (Refs. 8, 9).

For the general harmonic analysis, the atmospheric gust was considered as a random set of discrete gusts. Response had been predicted most commonly with the assumption that the vertical component of gust varied along the flight path, but did not vary along the span. This assumption was adopted by most researchers because the associated computations were less extensive than those for the more general cases of

random gusts. It may not be sufficiently accurate for very large aircraft, but it should provide useful data for most configurations.

Besides all these numerical calculations, not much experimental work appeared to have been done or to be available. Roberts and Hunt (Refs. 10, 11) made a series of measurements of transient pressures on a narrow delta wing of $AR=1.2$ due to vertical gusts, and Patel presented some experimental results for a couple of delta wings (Ref. 12) and other types of wings (Ref. 13) in harmonic gust fields.

In current aerodynamic research, the vortex flow phenomenon is drawing much attention because it offers significant contributions to aerodynamic characteristics on low-aspect-ratio wings with sharp or thin edges. For these types of configurations, the pressure distributions due to the leading-edge vortex separation are drastically different from those given by the conventional linear theory. The complex flowfield also makes it more difficult to predict aerodynamic forces accurately. Most of the aforementioned unsteady aerodynamic methods are based on the linear theory, and can not predict the leading-edge vortex effect. Although Atta, et al., (Ref. 14) developed an unsteady lifting-surface method with vortex flow by using the unsteady vortex-lattice method, no application to various gust problems has been presented and the computing cost is expected to be very expensive.

In this report, an unsteady lifting-surface method from reference 15 will be used to calculate the lift and pitching moment due to sinusoidal gusts for several wing planforms. The calculated results are compared with other theories for the attached flow and with experimental data for vortex flow. In calculating the response of a wing to a sharp-edged gust, Garrick (Ref. 16) developed a relation between the oscillatory forces due to flight

through continuous harmonic gusts and the indicial forces due to sharp-edged gusts. Instead of Fourier transform taken by most other theories in handling this reciprocal relationship, the present method will use Padé approximant to represent the harmonic response and Laplace transform will be used to calculate the indicial functions. The problem formulation and computed results are presented in the following chapters.

For many years, military personnel have been continuously interested in the prediction of the response of an aircraft resulting from a nuclear blast wave. Karman AviaDyne (Ref. 17) did a series of experiments to measure the blast pressures on a rigid highly sweptback wing at high subsonic speeds. McGrew, et al. (Refs. 18, 19) recently used the DLM to develop a nuclear blast response computer program for wing-body configurations. Yet the method is valid only for the attached flow. The present method, based on the unsteady suction analogy, will be used to demonstrate the capability of predicting the nuclear blast response involving the vortex flow. Some results in simulating experimental data in reference 17 will be shown.

2. MATHEMATICAL FORMULATION

2.1 Two-Dimensional Gust Penetration

Consider that a thin airfoil moving with a velocity U , enters a region of atmospheric gust with velocity distribution w_g normal to the direction of motion (see Fig. 1). The boundary condition requires that the total vertical velocity due to the gust and the vortex sheet simulating the airfoil must vanish:

$$w_g + w_a = 0; \quad \text{for } z = 0, -c^* \leq x \leq c^*, \quad (1)$$

where w_a is the vertical velocity component of the vortex sheet, x, z are the coordinate systems attached to the airfoil and c^* is the semichord length of the airfoil.

To solve a simple harmonic gust problem, the following expression is used to specify the sinusoidal gust:

$$w_g(x, t) = w_g^* e^{i\omega[t - (x/U)]}, \quad (2)$$

where w_g^* is the amplitude of w_g and ω is the radian frequency associated with the gust wavelength. Substituting into Eq. (1) and canceling out the time factor $e^{i\omega t}$, Eq. (2) leads to

$$w_a^*(x) = - w_g^* e^{-i\omega x/U}. \quad (3)$$

By way of introducing the reduced frequency, $k = \omega c^*/U$, Eq. (3) then becomes

$$w_a^*(x) = - w_g^* e^{-ik(x/c^*)}. \quad (4)$$

It is convenient to divide both sides by U and use the expression $\bar{x} = x/c^*$ as the non-dimensional x -coordinate,

$$\frac{w_a^*}{U} = - \frac{w_g^*}{U} e^{-ik\bar{x}},$$

$$\text{i.e., } \bar{w}_a = - \bar{w}_g e^{-ik\bar{x}}, \quad (5)$$

where $\bar{w}_a = w_a^* / U$ and $\bar{w}_g = w_g^* / U$.

Using Eq. (5), the exact lift distribution for incompressible flow can be shown to be (Ref. 20),

$$L = 2\pi\rho U c^* \bar{w}_g \{C(k)[J_0(k) - iJ_1(k)] + iJ_1(k)\} e^{i\omega t}, \quad (6)$$

where $C(k)$ is the Theodorsen's function, $J_0(k)$ and $J_1(k)$ are Bessel functions of the first kind. For compressible flow, $C(k)$ will be replaced by generalized Theodorsen's function** $C_c(k)$ and all other terms in Eq. (6) remain the same.

Furthermore, the lift caused by an arbitrary w_g can be calculated from Eq. (6). For a sharp-edged gust striking the leading edge of the airfoil at $t=0$, the boundary condition is

$$w_g = \begin{cases} 0, & x > Ut - c^*. \\ w_0, & x < Ut - c^*. \end{cases} \quad (7)$$

**The generalized Theodorsen's function was generated by Mr. Chung-Hao Hsu in his earlier work for calculating lift on wings due to step change in angle of attack.

Then, w_g can be represented by the Fourier integral,

$$w_g = \frac{1}{2\pi} \int_{-\infty}^{\infty} f(\omega) e^{i\omega t} d\omega, \quad (8)$$

which can be inverted into

$$f(\omega) = \int_{-\infty}^{\infty} w_g e^{-i\omega t} dt. \quad (9)$$

Since $w_g = 0$ for $t < \frac{x+c^*}{U}$, Eq. (9) can be shown to be, by following the Fourier transform of a constant (Ref. 20, p.287),

$$\begin{aligned} f(\omega) &= \int_{\frac{x+c^*}{U}}^{\infty} w_0 e^{-i\omega t} dt \\ &= \frac{w_0 e^{-i\omega(x+c^*)/U}}{i\omega}. \end{aligned} \quad (10)$$

Substituting Eq. (10) back into Eq. (8), the boundary condition for the sharp-edged gust becomes

$$\begin{aligned} w_g &= \frac{w_0}{2\pi} \int_{-\infty}^{\infty} \frac{e^{i\omega(t - \frac{c^*}{U} - \frac{x}{U})}}{i\omega} d\omega \\ &= \frac{w_0}{2\pi} \int_{-\infty}^{\infty} \frac{e^{ik(s - \bar{x} - 1)}}{ik} dk, \end{aligned} \quad (11)$$

where $s = Ut/c^*$ is the non-dimensional distance parameter. The airfoil

lift due to the harmonic gust (Eq. (5)) is given by Eq. (6). Therefore, for the step gust based on Eq. (11), the lift can be calculated as

$$L = \rho U c^* w_0 \int_{-\infty}^{\infty} \frac{\{C(k)[J_0(k) - iJ_1(k)] + iJ_1(k)\} e^{ik(s-1)}}{ik} dk. \quad (12)$$

From Eq. (12), the non-dimensional lift development due to a step gust, $\psi(s)$, is given by

$$L = 2\pi \rho U c^* w_0 \psi(s), \quad (13)$$

with

$$\psi(s) = \frac{1}{2\pi} \int_{-\infty}^{\infty} \frac{\{C(k)[J_0(k) - iJ_1(k)] + iJ_1(k)\} e^{ik(s-1)}}{ik} dk. \quad (14)$$

Let $F(k) = C(k)[J_0(k) - iJ_1(k)] + iJ_1(k)$, then

$$\begin{aligned} \psi(s) &= \frac{1}{2\pi} \int_{-\infty}^{\infty} \frac{F(k) e^{ik(s-1)}}{ik} dk \\ &= \frac{1}{2\pi} \int_{-\infty}^{\infty} \frac{F(k) e^{-ik}}{ik} e^{iks} dk. \end{aligned} \quad (15)$$

As k is always greater than or equal to zero, Eq. (15) can easily be inverted to

$$\frac{F(k) e^{-ik}}{ik} = \int_0^{\infty} \psi(s) e^{-iks} ds,$$

or

$$F(k) e^{-ik} = ik \int_0^{\infty} \psi(s) e^{-iks} ds. \quad (16)$$

Let $r = ik$. Then,

ORIGINAL PAGE IS
OF POOR QUALITY

$$\begin{aligned} F(k) e^{-r} &= r \int_0^{\infty} \psi(s) e^{-rs} ds \\ &= r \mathcal{L} \{ \psi(s) \}, \end{aligned} \quad (17)$$

$$\psi(s) = \mathcal{L}^{-1} \left\{ \frac{F(k) e^{-r}}{r} \right\}, \quad (18)$$

where $\mathcal{L} \{ \psi(s) \}$ is the Laplace transform of $\psi(s)$.

Hence, the indicial lift function can be obtained from the inverse Laplace transform involving the amplitude of lift distribution due to a sinusoidal gust.

2.2 Three-Dimensional Gust Penetration

Now consider a rigid thin wing travelling at speed U through an infinite array of harmonic gusts with vertical velocities w_g , uniformly across the wing span. The boundary condition is similar to that for a two-dimensional sinusoidal gust:

$$\bar{w}_a = - \bar{w}_g e^{-ik(x-x_R)/\bar{c}}, \quad (19)$$

where k again is the reduced frequency with a reference chord length \bar{c} , and x_R is a reference point for the gust phase.

Following reference 21, the oscillatory lift force due to the harmonic gust (Eq. (19)) is

$$L(t) = \rho U w_g S \{ L'(k) + i L''(k) \} e^{i\omega t}, \quad (20)$$

where S is the reference area of the wing, and $L'(k)$, $L''(k)$ are the in-phase and out-of-phase components of the dimensionless lift force.

Next consider a wing entering a sharp-edged gust. Again the boundary condition is very similar to Eq. (7),

$$w_g = \begin{cases} 0, & x > Ut + x_{le}, \\ w_0, & x < Ut + x_{le}, \end{cases} \quad (21)$$

where x_{le} is the x -coordinate of the leading-edge of the wing. From Eq. (20), one can determine the indicial lift function representing dimensionless lift development due to a step gust, $\psi(s)$,

$$L(s) = \rho U w_0 S \psi(s), \quad (22)$$

with

$$\psi(s) = \frac{1}{2\pi} \int_{-\infty}^{\infty} \left(\frac{L'(k) + iL''(k)}{ik} \right) e^{iks} dk. \quad (23)$$

Let

$$T(k) = L'(k) + iL''(k), \quad (24)$$

$$\psi(s) = \frac{1}{2\pi} \int_{-\infty}^{\infty} \frac{T(k)}{ik} e^{iks} dk. \quad (25)$$

With the same procedures from Eqs. (15) - (18), $\psi(s)$ can be obtained from the inverse Laplace transform involving the dimensionless lift distribution due to a harmonic gust,

$$\psi(s) = L^{-1} \left\{ \frac{T(k)}{r} \right\}. \quad (26)$$

2.3 Padé Approximant

To be able to calculate the inverse Laplace transform indicated in Eqs. (18) and (26), it is convenient to express $T(k)$ and $F(k)e^{-r}$ as closed-form functions of r . In any lifting-surface computation, $T(k)$ or $F(k)$ are calculated only at a finite number of k 's. These values can then be interpolated by Padé approximant as suggested by Vepa (Ref. 22). Following Vepa, an $[N,N]$ sequence of Padé approximant to approximate $T(k)$ in three-dimensional case and $F(k)e^{-r}$ in two-dimensional gust can be written as,

$$T(k) = 1 - [N,N], \quad F(k)e^{-r} = 1 - [N,N], \quad (27)$$

$$[N,N] = \frac{A_0 r^N + A_1 r^{N-1} + \dots + A_{N-1} r}{r^N + A_N r^{N-1} + \dots + A_{2N-1}}, \quad (28)$$

where A_i are the coefficients of Padé approximant.

For $N = 3$ and use $T(k)$ as an example,

$$T(k) = 1 - \frac{A_0 r^3 + A_1 r^2 + A_2 r}{r^3 + A_3 r^2 + A_4 r + A_5}, \quad (29a)$$

and for $N = 2$,

$$T(k) = 1 - \frac{A_0 r^2 + A_1 r}{r^2 + A_2 r + A_3}. \quad (29b)$$

Let

$$1 - T(k) = V(k) + iW(k). \quad (30)$$

From Eq. (30), it follows that for $N = 3$,

$$V(k) + iW(k) = \frac{A_0(ik)^3 + A_1(ik)^2 + A_2(ik)}{(ik)^3 + A_3(ik)^2 + A_4(ik) + A_5} \quad (31)$$

Eq. (31) can be expanded and separated into real and imaginary parts respectively to give,

real part:

$$A_1 k^2 - A_3 V k - A_4 W k + A_5 V + W k^3 = 0, \quad (32a)$$

imaginary part:

$$A_0 k^3 - A_2 k - A_3 W k + A_4 V k + A_5 W - V k^3 = 0. \quad (32b)$$

Normally, more values of k 's are chosen to calculate $T(k)$ than the number of unknowns A_i in Eq. (32a) and (32b). Therefore, a least square technique to be described next is used to determine A_i 's.

2.4 Least Square Technique

The least square principle is based on the requirements that A_i 's are determined by minimizing the sum of squares of errors:

$$\text{Sum} = \sum_{1}^M (\text{L.H.S. of Eq. (32a)})^2 + \sum_{1}^M (\text{L.H.S. of Eq. (32b)})^2 \quad (33)$$

where M is the number of k 's of which $T(k)$ is calculated by any existing lifting-surface theory.

At a minimum, all the partial derivatives with respect to A_i 's, such as $\partial \text{Sum} / \partial A_0$, $\partial \text{Sum} / \partial A_1$, ..., $\partial \text{Sum} / \partial A_5$, must vanish. These conditions result in $i+1$ equations for $i+1$ unknown coefficients A_i 's. Thus, A_i 's can be solved from Eq. (33) with M different lift values at corresponding k 's.

2.5 Indicial Lift Function

After all coefficients of the Padé approximant are determined, Eq. (29a) can be rewritten as,

$$\tau(k) = 1 - r \frac{A_0 r^2 + A_1 r + A_2}{r^3 + A_3 r^2 + A_4 r + A_5} . \quad (34)$$

By partial fraction method, Eq. (34) leads to

$$\frac{\tau(k)}{r} = \frac{1}{r} - \sum_{i=1}^3 \frac{B_i}{r - \beta_i} , \quad (35)$$

where β_i is the i th root of the polynomial in the denominator of Eq. (34) and B_i is the corresponding coefficient of partial fraction in Eq. (35).

Based on Eq. (26), the indicial lift function $\psi(s)$ can be obtained by applying the inverse Laplace transform to Eq. (35),

$$\psi(s) = 1 - \sum_{i=1}^3 B_i e^{\beta_i s} . \quad (36)$$

2.6 Nuclear Blast Response

Calculation of the lift development of a thin wing encountering a nuclear blast wave will follow the same way as in computing the sharp-edged gust response. No major change has to be made except the boundary condition. The shock wave induced by the nuclear blast is assumed traveling at sonic speed. Thus, an impulse function $\delta(s)$ is used instead of the unit step function in the gust response condition (Ref. 24),

$$w_g = w_0 \delta\left(t - \frac{x - x_1}{U}\right) . \quad (37)$$

where \bar{U} is the magnitude of the vector sum of the shock wave velocity and the freestream velocity. Eq. (9) now becomes,

$$\begin{aligned} f(\omega) &= \int_{-\infty}^{\infty} w_0 \delta\left(t - \frac{x - x_1 e}{\bar{U}}\right) e^{-i\omega t} dt \\ &= w_0 e^{-i\omega \left(\frac{x - x_1 e}{\bar{U}}\right)}. \end{aligned} \quad (38)$$

Comparing Eq. (38) with Eq. (10), the main difference is the factor " $i\omega$ " in the denominator of Eq. (10). This also follows from the fact that the impulse is equal to the time derivative of the step input. Hence,

$$F\{h(t)\} = i\omega F\{A(t)\}, \quad (39)$$

where $h(t)$ is the unit impulse, $A(t)$ is the step function and $F\{\}$ is the Fourier transform.

Rewriting Eq. (25) for the impulse response, it follows that,

$$h(s) = \frac{1}{2\pi} \int_{-\infty}^{\infty} T(k) e^{iks} dk, \quad (40)$$

or,

$$h(s) = L^{-1}\{T(k)\}. \quad (41)$$

The Padé approximant used for the indicial response analysis remains applicable, except the inverse transform calculation has changed. For example, $N=2$ Padé approximant can be written as,

$$T(k) = 1 - \frac{A_0 r^2 + A_1 r}{r^2 + A_2 r + A_3}$$

$$= 1 - \left[A_0 + \frac{(A_1 - A_0 A_2)r - A_0 A_3}{r^2 + A_2 r + A_3} \right]$$

ORIGINAL FILED BY
OF POOR QUALITY

$$= 1 - A_0 - \sum_{i=1}^2 \frac{B_i}{r - \beta_i} . \quad (42)$$

From Eq. (41), the impulse lift function $h(s)$ can obtained,

$$\begin{aligned} h(s) &= \mathcal{L}^{-1} \{ T(k) \} \\ &= (1 - A) \delta(s) - \sum_{i=1}^2 B_i e^{\beta_i s} . \end{aligned} \quad (43)$$

3. NUMERICAL RESULTS AND DISCUSSIONS

3.1. Gust Penetration

3.1.1. Sinusoidal gust problem

The lift development due to a harmonic gust is calculated by the computer program based upon the unsteady quasi-vortex-lattice method developed by Lan (Ref. 23).

For a thin airfoil, 30 vortex elements are used in the computation. The steady state two-dimensional lift values are simply calculated by the equation $C_{l_0} = 2\pi/\beta$, where $\beta = \sqrt{1-M^2}$, M is the freestream Mach number. The computed results are compared with Sears' for incompressible flow and with Graham's for several different Mach numbers at reduced frequency 2. Both comparisons, showing good agreement, are tabulated in Tables I and II.

The three-dimensional unsteady aerodynamic program of reference 15 is then revised to account for the gust response. The present attached flow results of lift and moment for a delta wing of 75° sweep at $M = 0.4$ are compared in Figs. 2 and 3 with those calculated by a kernel function method (Ref. 5).

Results of calculation will also be compared with experimental data. In references 12 and 13, a gust tunnel which could generate a sinusoidal vertical gust was used to measure the oscillatory lift and moment on two delta wings of $AR=1$ and 2 , and several other commonly used wing planforms. The tests were performed for all wings at two mean freestream velocities of 12.43 and 20.00 m/s. However, the oscillatory gust waves convected downstream with a velocity of 0.61 of the mean freestream velocity. This would indeed influence the gust wavelength, i.e., the frequency parameter. Thus, in the present calculations based on gust moving with the freestream

velocity, an effective frequency ($k' = k/0.61$), as suggested by Patel, will be used in the following comparisons.

In Fig. 4, test data for a rectangular wing of $AR = 6$ (Ref. 13) are compared with two sets of theoretical results. It is seen that the present theory agrees well with Graham's (Ref. 24) in the predicted in-phase component of the oscillatory lift. The phase lag is underpredicted and both theories overpredict the lift amplitude.

To demonstrate the vortex flow effect, a delta wing of $AR=1$ is used to compare with Patel's data (Ref. 12) at $\alpha = 0$ and 12 degrees in Fig. 5. The present theory predicts well the lift amplitude at both angles of attack. At $\alpha = 12^\circ$, the phase lag is also adequately predicted by the present theory. On the other hand, the phase lag at $\alpha = 0^\circ$ is not accurately predicted. In seeking the reasons for these deviations, several points should be noted:

(1) At $\alpha = 0$ degree, the attached flow prevails. It is of interest to compare the present results with the doublet-lattice method (Refs. 8,9) for this delta wing of $AR=1$. In Fig. 6, agreement between the present results and doublet-lattice method's is excellent in lift amplitude and phase angles.

(2) As depicted in reference 12, force measurements were made relative to the undisturbed freestream gust at the root 2/3rd chord point. Another point at the gust tunnel exit was also used as a reference. It is not known whether the conditions at the exit point were disturbed once the test model was placed in the tunnel.

(3) Also, Patel indicated in reference 12 from test data that the incremental lift due to vortex lift contribution was important in magnitude only with no measurable contribution to phase angles. However, the

present theory shows that this is approximately true only with respect to some reference points [i.e., x_R at Eq. (19)]. This is illustrated in Fig. 7 with the root midchord point and wing apex as reference points. Therefore, the results by the present theory very much depend on the precise location of the reference about which the phase angle is calculated.

At any rate, reasons for the discrepancy in the predicted phase angles at $\alpha = 0$ degree for the delta wing of $AR = 1$ are still unknown at the present time.

3.1.2. Padé approximant

Two different sequences of Padé approximant are constructed here to fit various freestream conditions. For airfoils in compressible flows, Padé approximant with $N = 3$ in Eq. (27) (called Padé A6) is used. On the other hand, Padé approximant with $N = 2$ (called Padé A3) is used for airfoils in incompressible flow and also for three-dimensional conditions. These choices are made through numerical correlations. The corresponding matrices for deciding the unknown coefficients A_i in Eq. (28) are presented in Appendix A.

The good agreement between the calculated results from the unsteady QVLM and by Padé approximant for a thin airfoil in the harmonic gust is shown in Fig. 8 for incompressible flow, Fig. 9 for Mach 0.5 and Fig. 10 for Mach 0.7. The oscillatory lift for a delta wing of $AR = 1.2$ to be used for calculating step gust response is shown in Figs. 11 and 12 for upward and downward gust respectively.

Most other theories use Fourier transform to handle the reciprocal relationship between the oscillatory and indicial lift forces. So they need harmonic lift values at a large number of different frequencies.

But the number of k required by the present method is only 7 (including $k=0$), and the indicial lift results, which will be seen in the next section, still show good accuracy.

3.1.3. Indicial lift function

The indicial lift results performed by using the inverse Laplace transform described in the preceding chapter will be presented. First, for a thin airfoil passing through step gusts in incompressible and compressible flows, Fig. 13 shows plots for Küssner function, and Figs. 14, 15 exhibit the indicial lift at Mach 0.5 and 0.7. Good results have been expected because of the accurate approximant shown in last section. The exact solutions are calculated through the data in Table 6-2 of reference 20. From Fig. 16, it is apparent that the compressibility effect decreases the rate of lift build-up in two-dimensional flow.

Second, in thin wing gust penetration, for lack of experimental force data to make a direct comparison, some pressure data (Ref. 11) will be employed to compare the trend produced by calculated total lift.

The configuration of the delta wing used in reference 11 is shown in Fig. 17(a). The model wing was carried along a straight railway track on a rocket-propelled sledge, through the efflux from an open-jet wind tunnel blowing across the track. The velocity of the sledge was 180 ft/sec., the tunnel efflux velocity was 47 ft/sec., and the model was at zero angle of attack. For measurements of transient pressure, four transducers were positioned at locations being 0.3, 0.4, 0.5, 0.6 root chords aft of the apex, and along a line at 75% semispan [see Fig. 17(a)]. In accordance with figures in reference 11, the indicial lift is plotted against local distance parameters x_n/b_n in comparing with pressure values through

transducers A, B and C, where x_n and b_n are defined in Fig. 17(b).

Fig. 18 shows the similar trend between measured transient pressure and the calculated indicial lift for both upward and downward sharp-edged gust. It is seen that the development of a gust-induced gain of lift is very gradual. On the contrary, the gust-induced loss of lift occurs relatively instantly. In the calculations, the vortex lag described in reference 15 is assumed to be present if the lift is increasing and there is no vortex lag if the lift is decreasing. This assumption appears to be reasonably accurate for the leading-edge vortex flow. This can also be seen from Fig. 19 which illustrates the comparisons among the vortex flow and potential results. There is some significant difference for the upward gust while the trend is quite close in the downward gust condition.

3.2. Nuclear Blast Response

The unsteady aerodynamic program of reference 15 is again used to calculate the nuclear blast responses of aircraft flying at high subsonic speeds.

Reference 17 is the only obtainable test data which can be used to check the leading-edge vortex separation effect, predicted by the present method, on aircraft nuclear blast response. The sideview of a thin wing intercepted by nuclear blast waves is shown in Fig. 20. Fig. 21 shows the test model which consists of a swept wing of 67° leading-edge sweptback angle with a nose and partial fuselage section. In the test, the model was mounted on a high speed dual rail rocket sled at an initial angle of attack of 3.2° . The sled, travelling at Mach 0.76, was intercepted progressively by blast waves from sequential detonation of charges of TNT with the blast intercept angle $\theta = 20^\circ$ (see Fig. 20). Twenty pairs of

pressure transducers were installed on the left wing half to measure the blast-induced pressures.

For the purpose of correlation with the test model, a semiwing used by the present method is illustrated in Fig. 22. For such a configuration, the concept of augmented lift is included in the present calculation. The definition for the characteristic length is adopted from reference 26. With negative augmented vortex lift, the vortex lift effect may not be as strong as expected even the leading-edge sweptback angle is 67° for the test model.

Fig. 23, reproduced from reference 17, shows the pressure variation measured by transducer 13 which was positioned at half semispan and along quarter chord line. Like DLM, the present theory underpredict the blast-induced incremental pressure loadings because the nonlinear vortex effect is not included in the calculation of pressure differential. The present theory, being based on unsteady suction analogy, can only demonstrate the vortex effect by the variation of total lift or moment. Fig. 24 shows the comparison of vortex flow with attached flow for impulse lift. It is evident that the vortex lag decreases the rate of lift decay after the blast intercept.

There are several factors which must be mentioned in connection with Figs. 23 and 24:

- (1) The blast amplitude is determined by peak material velocity (gust) behind the shock front and is assumed invariant throughout the present calculation.

- (2) In the experiment, because of different locations of transducers, the blast intercept time (time at the shock arrival) is different for each transducer. In the present calculation, the coordinate origin is set at the apex of the wing, so that the intercept is exactly at $s=0$ as

shown in Fig. 24. However, to correlate with the test data, a shift has been made in Fig. 23.

(3) The steady state lift value is used for all time parameters less than zero since there is no incremental lift or pressure differential values for $s < 0$ in the present analytical results.

For a more significant vortex lift effect, the impulse lift on a delta wing of $AR = 2$ at Mach 0.5 intercepted by a blast wave with the same intercept angle as that in Fig. 20 is considered. The initial angle of attack is assumed to be 15° and the peak blast-induced angle of attack is assumed to be an additional 15° . The attached-flow oscillatory lift can be well represented by a Padé approximant as indicated in Fig. 25. However, with the vortex lift effect included, the Padé approximant fails to approximate the calculated results accurately as shown in Fig. 26. Because of this reason, the calculation of impulse lift for this delta wing was not successful; and hence, the results are not presented here.

4. CONCLUSIONS AND RECOMMENDATIONS

An unsteady lifting-surface computer program based on quasi-vortex-lattice method along with leading-edge suction analogy has been developed to estimate the oscillatory air forces on wings of general planforms in gust flow at any frequency. Padé approximant and Laplace transform have made it practical to convert the oscillatory air forces to indicial air forces.

Both the experimental data and other theoretical results are used to check the accuracy of the present calculations in attached flow and with vortex lift effect. It is shown that the present method can accurately predict the oscillatory and indicial lift on wings in different gust fields. Also, the phenomenon of the gust-induced gain of lift being very gradual and the gust-induced loss of lift occurring relatively abruptly can be explained by the presence or absence of vortex lag effect.

The present program is extended to account for the nuclear blast response as well. Though there is no lift data available at this time, the trend for the vortex lag is clearly seen from the comparison between the attached flow and vortex results predicted by the present method.

The following points should be noted to improve the efficiency and capability of the present method.

(1) In the present calculations, 72 vortex elements were used for half wingspan - 6 in the chordwise direction and 12 in the spanwise direction. It is recommended that 40 elements (e.g., 4 in the chordwise direction, 10 in the spanwise direction) could be used in lieu of 72 for small reduced frequencies; thus, the size of the aerodynamic influence coefficient matrix could be greatly reduced.

(2) The present method can only deal with nuclear blast locations being on the plane of symmetry, i.e., the X-Y plane. For more general blast orientations, the present method should be extended to calculate the aircraft wing response of the blast waves coming from any arbitrary direction, since an asymmetric condition can always be treated as a combination of a symmetric and an antisymmetrical conditions.

(3) Among the existing approximation schemes for the unsteady aerodynamic loads, Karpel's approximant (Ref. 28) provides better accuracy than Fadé's. It is suggested the present method should include more than one approximant to meet different gust and blast conditions.

5. REFERENCES

1. Von Kármán, T., and Sears, W. R., "Airfoil Theory for Nonuniform Motion", *Journal of the Aeronautical Sciences*, Vol. 5, No. 10, Aug., 1938, pp. 379-390.
2. Miles, J. W., "The Aerodynamic Forces on an Airfoil in a Moving Gust", *Journal of the Aeronautical Sciences*, Vol. 23, No. 11, Nov. 1956, pp. 1044-1050.
3. Drischler, J. A., and Diederich, F. W., "Lift and Moment Responses to Penetration of Sharp-Edged Travelling Gusts, with Application to Penetration of Weak Blast Waves", NACA Tech. Rep. 3958, May 1957.
4. Sears, W. R., "Some Aspects of Non-Stationary Airfoil Theory and Its Practical Application", *Journal of the Aeronautical Sciences*, Vol. 8, No. 3, Jan. 1941, pp. 104-108.
5. Murrow, H. N., et al. "Numerical Technique to Lifting-Surface Theory for Calculation of Unsteady Aerodynamic Forces due to Continuous Sinusoidal Gusts on Several Wing Planforms", NASA TN D-1501, Feb. 1963.
6. Giesing, J. P., Rodden, W. P., and Stahl, B., "Sears Function and Lifting Surface Theory for Harmonic Gust Fields", *Journal of Aircraft*, Vol. 7, No. 3, May - June, 1970, pp. 252-255.
7. Albano, E., and Rodden, W. P., "A Doublet-Lattice Method for Calculating Lift Distributions on Oscillating Surfaces in Subsonic Flows", *AIAA Journal*, Vol. 7, No. 2, Feb. 1969, pp. 279-285.
8. Giesing, J. P., Kalman, T. P., and Rodden, W. P., "Subsonic Unsteady Aerodynamics for General Configurations; Part I - Direct Application of the Nonplanar Doublet-Lattice Method", Air Force Flight Dynamics Laboratory, Report No. AFFDL-TR-71-5, Part I, Nov. 1971.
9. Giesing, J. P., Kalman, T. P., and Rodden, W. P., "Subsonic Unsteady Aerodynamics for General Configurations; Part II - Application of the Doublet-Lattice Method and the Method of Images to Lifting-Surface/Body Interference", Air Force Flight Dynamics Laboratory, Report No. AFFDL-71-TR-5, Part II, April 1972.
10. Roberts, D. R., Hunt, G. K., and Walker, D., "Measurements of Transient Pressures on a Narrow-Delta Wing due to an Upward Gust", ARC C. P., No. 624, 1961.
11. Roberts, D. R., and Hunt, G. K., "Further Measurements of Transient Pressures on a Narrow-Delta Wing due to a Vertical Gust", ARC C. P., No. 7012, 1966.

12. Patel, M. H., "The Delta Wing in Oscillatory Gusts", *AIAA Journal*, Vol. 18, No. 5, May 1980, pp. 481-486.
13. Patel, M. H., "Aerodynamic Forces on Finite Wings in Oscillatory Flows: An Experimental Study", *AIAA Journal*, Vol. 16, No. 11, Nov. 1978, pp. 1175-1180.
14. Atta, E. H., et al., "Unsteady Aerodynamic Loads on Arbitrary Wings Including Wing-Tip and Leading Edge Separation", AIAA Paper 77-156, 1977.
15. Lan, C. E., "The Unsteady Suction Analogy and Applications", *AIAA Journal*, Vol. 20, No. 12, Dec. 1982, pp. 1647-1656.
16. Garrick, I. E., "On Some Fourier Transforms in the Theory of Non-Stationary Flows", NACA Report No. 629, 1938.
17. Zartarian, G., Ruetenik, J. R., and Smiley, R. F., "Measurements of Blast Pressures on a Rigid Wing at Mach 0.76 from Rocket Propelled Sled Tests; Vol. III - Correlation with the Doublet-Lattice Method in VIBRA-6", Defense Nuclear Agency, Report No. DNA 4400F-3, Dec. 1977.
18. McGrew, et al., "Nuclear Blast Response Computer Program; Vol. I - Program Description", Air Force Weapons Laboratory, Report No. AFWL-TR-81-32, Vol. I, Aug. 1981.
19. McGrew, et al., "Nuclear Blast Response Computer Program; Vol. II - Doublet-Lattice and Piston Theory Aerodynamics", Air Force Weapons Laboratory, Report No. AFWL-TR-81-32, Vol. II, Aug. 1981.
20. Bisplinghoff, R. L., Ashley, H., and Halfman, R. L., *Aeroelasticity*, Chapter 5, 6, Addison-Wesley, Cambridge, Mass., 1955.
21. Mitchell, C. G. B., "The Calculation of Aerodynamic Forces and Pressures on Wings Entering Step Gusts", *The Aeronautical Journal*, Vol. 72, No. 689, May 1968, pp. 535-539.
22. Vepa, R., "Finite State Modeling of Aeroelastic Systems", NASA CR-2779, Feb. 1977.
23. Lan, C. E., "The Induced Drag of Oscillating Airfoils in Linear Subsonic Compressible Flow", University of Kansas, Report No. KU-FRL-400, 1975.
24. Graham, J. M. R., "A Lifting Surface Theory for the Rectangular Wing in Non-Stationary Flow", *Aeronautical Quarterly*, Vol. 22, Feb. 1971, pp. 83-100.
25. Zartarian, G., "Application of the Doublet-Lattice Method for Determination of Blast Loads on Lifting Surfaces at Subsonic Speeds", Air Force Weapons Laboratory, Report No. AFWL-TR-72-207, Jan. 1973.

26. Lamar, J. E., "Recent Studies of Subsonic Vortex Lift Including Parameters Affecting Stable Leading Edge Vortex Flow", *Journal of Aircraft*, Vol. 14, No. 12, Dec. 1977, pp. 1205-1211.
27. Kemp, N. H., "On the Lift and Circulation of Airfoils in Some Unsteady Flow Problems", Reader's Forum, *Journal of the Aeronautical Sciences*, Vol. 19, No. 10, Oct. 1952, pp. 713-714.
28. Karpel, M., "Design for Active Flutter Suppression and Gust Alleviation Using State-Space Aeroelastic Modeling", AIAA Paper 80-0766, May, 1980.

ORIGINAL PAGE IS
OF POOR QUALITY

ORIGINAL PAGE IS
OF POOR QUALITY

Table I. Oscillatory Lift* on an Airfoil in Sinusoidal Gusts at $M = 0$.

| k | Present Method | | Sears' ** | |
|------|-----------------|-----------------|-----------------|-----------------|
| | C_{lr}/C_{l0} | C_{li}/C_{l0} | C_{lr}/C_{l0} | C_{li}/C_{l0} |
| 0.02 | 0.96289 | -0.07484 | 0.963 | -0.075 |
| 0.04 | 0.92403 | -0.11449 | 0.924 | -0.114 |
| 0.06 | 0.88697 | -0.13923 | 0.887 | -0.139 |
| 0.08 | 0.85266 | -0.15457 | 0.852 | -0.154 |
| 0.10 | 0.82126 | -0.16348 | 0.821 | -0.164 |
| 0.20 | 0.70156 | -0.15964 | 0.702 | -0.160 |
| 0.40 | 0.56789 | -0.08494 | 0.568 | -0.085 |
| 0.60 | 0.48837 | -0.00490 | 0.488 | -0.005 |
| 1.00 | 0.36865 | 0.12594 | 0.369 | 0.126 |
| 2.00 | 0.08158 | 0.26796 | 0.082 | 0.268 |

* C_{lr} and C_{li} are the in-phase and out-of-phase components.

** Sears' results are copied from reference 27.

ORIGINAL PAGE IS
OF POOR QUALITY

Table II. Oscillatory Lift on an Airfoil in Sinusoidal
Gust at $k = 2.0$.

| M | Present Method | | Graham's | |
|-----|----------------|----------|----------|----------|
| | C_{lr} | C_{li} | C_{lr} | C_{li} |
| 0.0 | 0.5126 | 1.6836 | 0.5125 | 1.6837 |
| 0.2 | 0.6925 | 1.7473 | 0.6955 | 1.7441 |
| 0.4 | 1.1535 | 1.5960 | 1.1511 | 1.5953 |
| 0.5 | 1.2773 | 1.3139 | 1.2774 | 1.3138 |
| 0.6 | 1.2138 | 1.1104 | 1.2139 | 1.1102 |
| 0.7 | 1.2192 | 1.0113 | 1.2152 | 1.0085 |
| 0.8 | 1.1881 | 0.8921 | 1.1838 | 0.8897 |
| 0.9 | 1.1516 | 0.7986 | 1.1486 | 0.7961 |

*The results correspond to $\bar{w}_g = 1$ in Eq. (4).

**Graham's results are taken from reference 23.

APPENDIX A Coefficient Matrices of Padé Approximation with Least Square Techniques

1. Padé A 6 (3,3)

ORIGINAL PAGE IS
OF POOR QUALITY

$$\begin{pmatrix} \Sigma k_j^6 & 0 & -\Sigma k_j^4 & -\Sigma k_j^5 W_j & \Sigma k_j^4 U_j & \Sigma k_j^3 W_j \\ 0 & \Sigma k_j^4 & 0 & -\Sigma k_j^3 U_j & -\Sigma k_j^3 W_j & \Sigma k_j^2 U_j \\ \Sigma k_j^4 & 0 & -\Sigma k_j^2 & -\Sigma k_j^3 W_j & \Sigma k_j^2 U_j & \Sigma k_j W_j \\ \Sigma k_j^5 W_j & \Sigma k_j^4 U_j & -\Sigma k_j^3 W_j & -\Sigma k_j^4 (U_j^2 + W_j^2) & 0 & \Sigma k_j^2 (U_j^2 + W_j^2) \\ \Sigma k_j^4 U_j & -\Sigma k_j^2 W_j & -\Sigma k_j^2 U_j & 0 & \Sigma k_j^2 (U_j^2 + W_j^2) & 0 \\ \Sigma k_j^3 W_j & \Sigma k_j^2 U_j & -\Sigma k_j W_j & -\Sigma k_j^2 (U_j^2 + W_j^2) & 0 & \Sigma (U_j^2 + W_j^2) \end{pmatrix} \begin{pmatrix} A_0 \\ A_1 \\ A_2 \\ A_3 \\ A_4 \\ A_5 \end{pmatrix} = \begin{pmatrix} \Sigma k_j^6 U_j \\ -\Sigma k_j^5 W_j \\ \Sigma k_j^4 U_j \\ 0 \\ \Sigma k_j^4 (U_j^2 + W_j^2) \\ 0 \end{pmatrix}$$

2. Padé A 3 (2,2)

$$\begin{pmatrix} \Sigma k_j^4 & 0 & -\Sigma k_j^3 W_j & \Sigma k_j^2 U_j \\ 0 & \Sigma k_j^2 & -\Sigma k_j^2 U_j & -\Sigma k_j W_j \\ -\Sigma k_j^3 W_j & -\Sigma k_j^2 U_j & \Sigma k_j^2 (U_j^2 + W_j^2) & 0 \\ \Sigma k_j^2 U_j & -\Sigma k_j W_j & 0 & \Sigma (U_j^2 + W_j^2) \end{pmatrix} \begin{pmatrix} A_0 \\ A_1 \\ A_2 \\ A_3 \end{pmatrix} = \begin{pmatrix} \Sigma k_j^4 U_j \\ -\Sigma k_j^3 W_j \\ 0 \\ \Sigma k_j^2 (U_j^2 + W_j^2) \end{pmatrix}$$

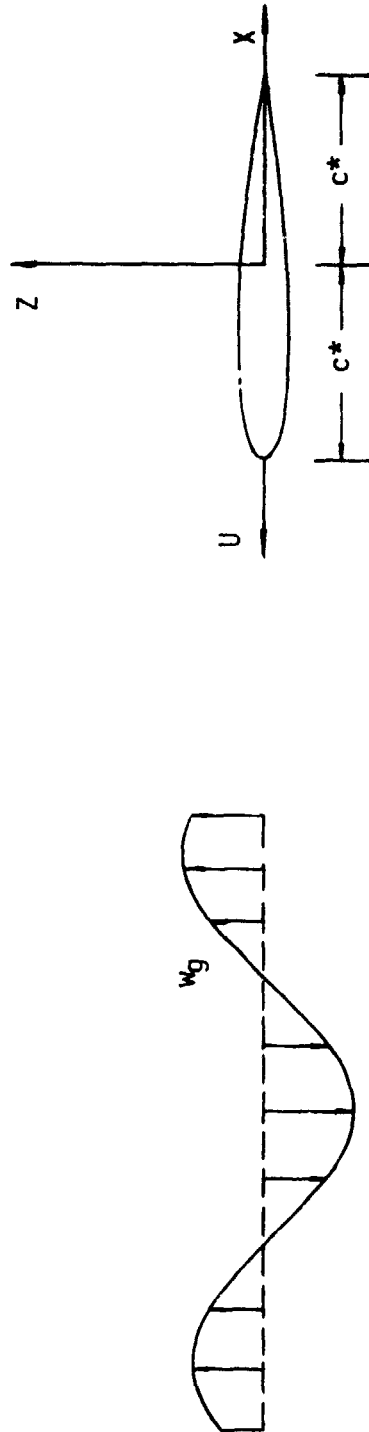


Fig. 1 Thin airfoil passing through a region of harmonic gusts with vertical gust velocity distribution $w_g(x, t)$.

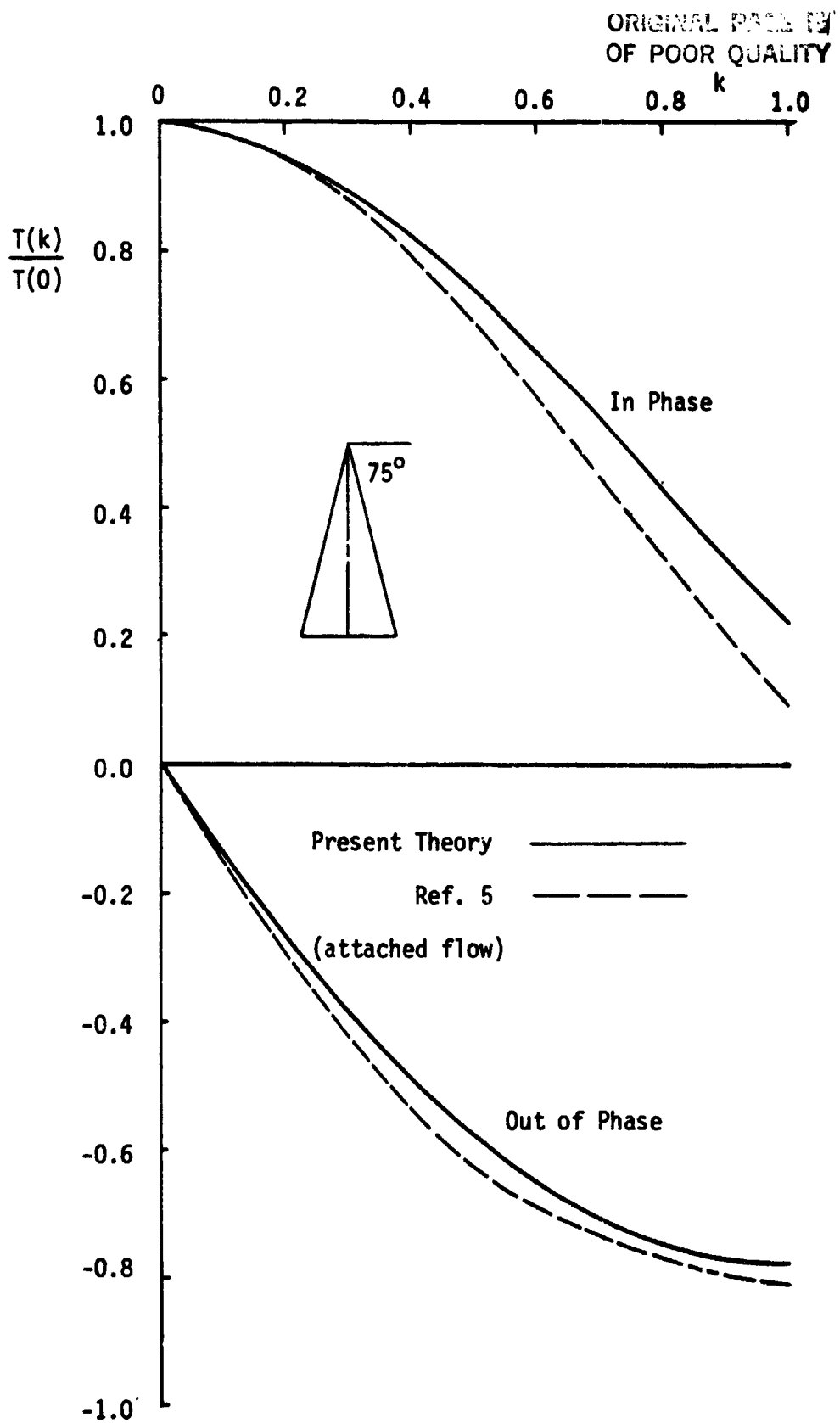


Fig. 2 Generalized oscillatory lift for a 75° delta wing due to harmonic gusts with $\bar{w}_g = 1$ at $M = 0.4$.

ORIGINAL PAGE IS
OF POOR QUALITY

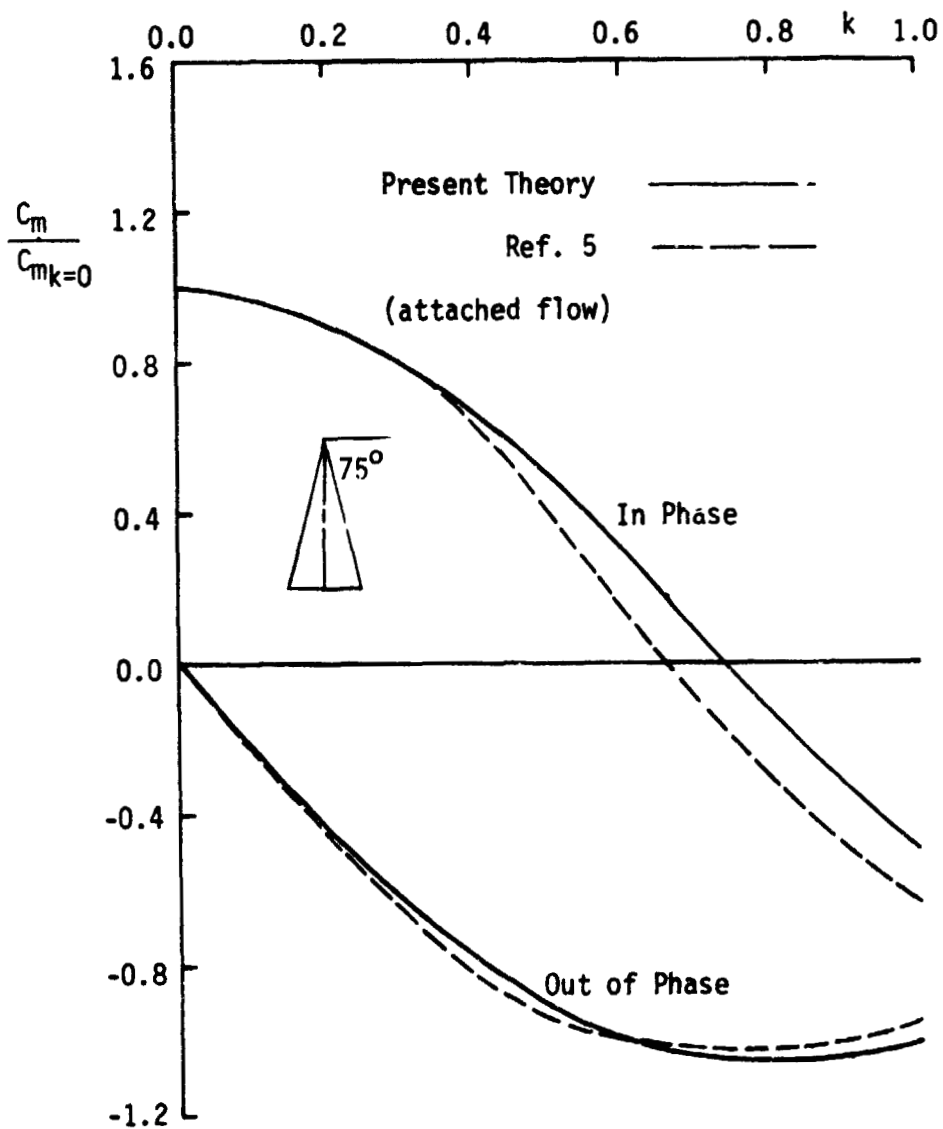


Fig. 3 Generalized oscillatory pitching moment for a 75° delta wing due to harmonic gusts with $\bar{w}_g = 1$ at $M = 0.4$; pitching axis at root midchord point.

ORIGINAL PAGE IS
OF POOR QUALITY

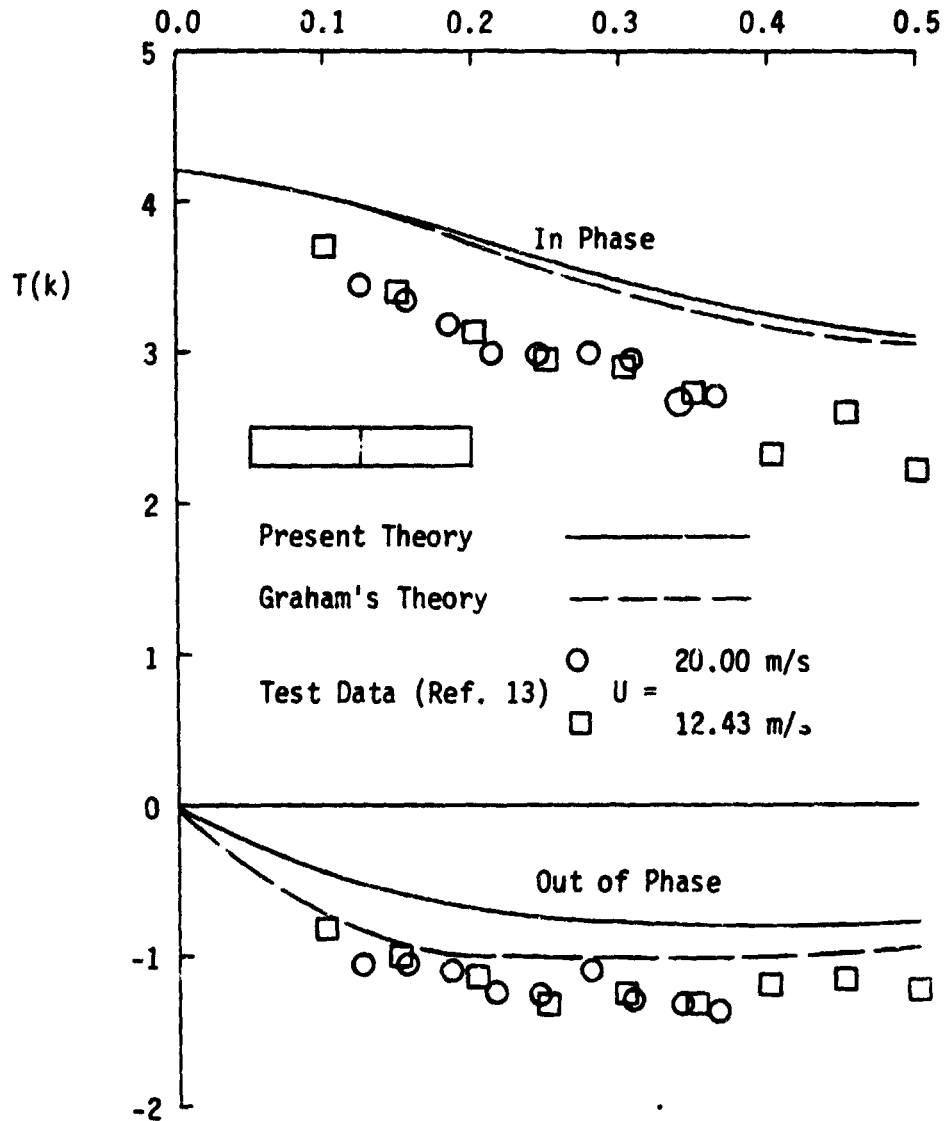


Fig. 4 Incremental lift for a rectangular wing of $AR = 6$ due to sinusoidal gusts for $\alpha = 0^\circ$ with $\bar{w}_g = 0.0314$ and reference point at root quarter chord point.

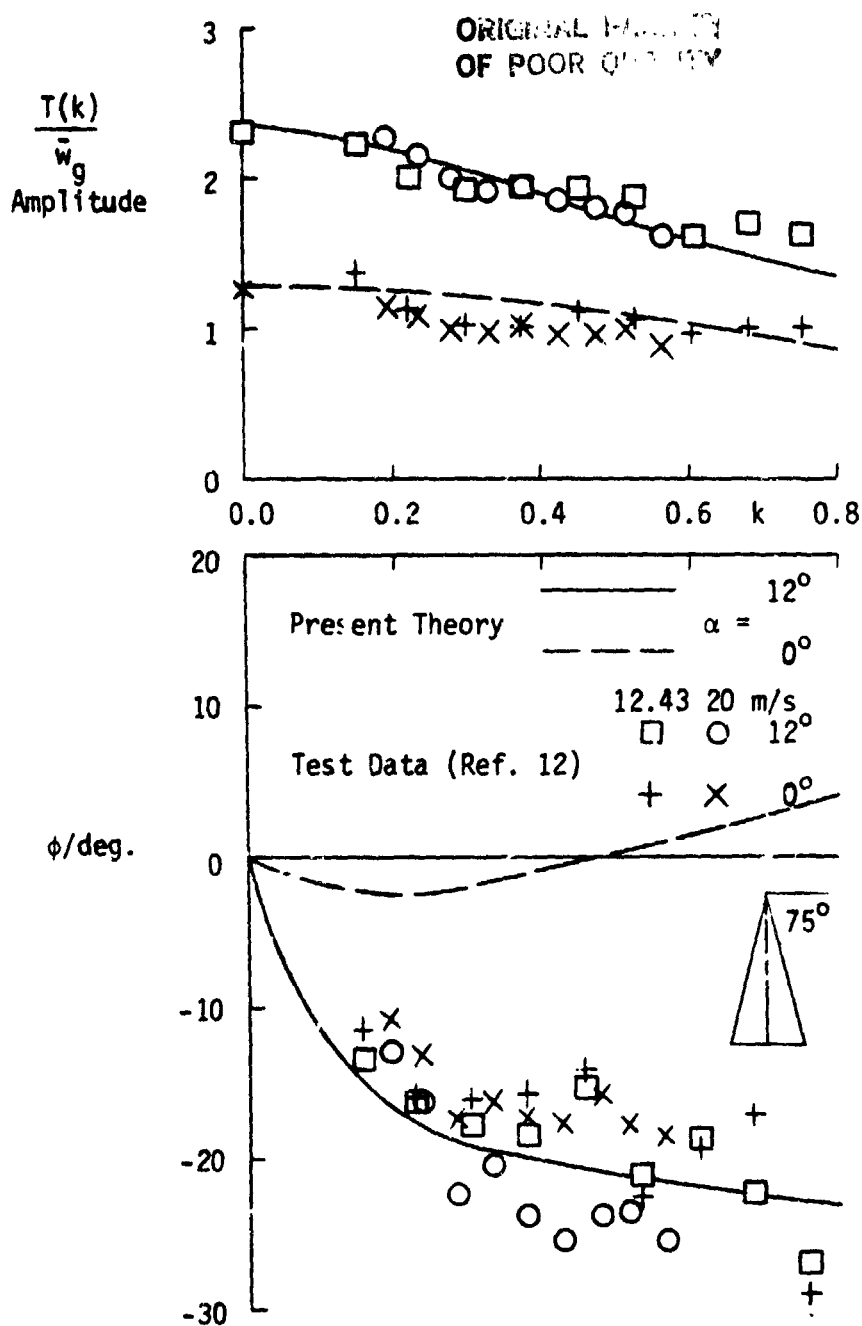


Fig. 5 Incremental lift for a delta wing of $AR = 1$ in sinusoidal gusts for $\alpha = 0$ and 12 degrees with $\bar{w}_g = 0.0314$ and reference point at root $2/3$ rd chord point.

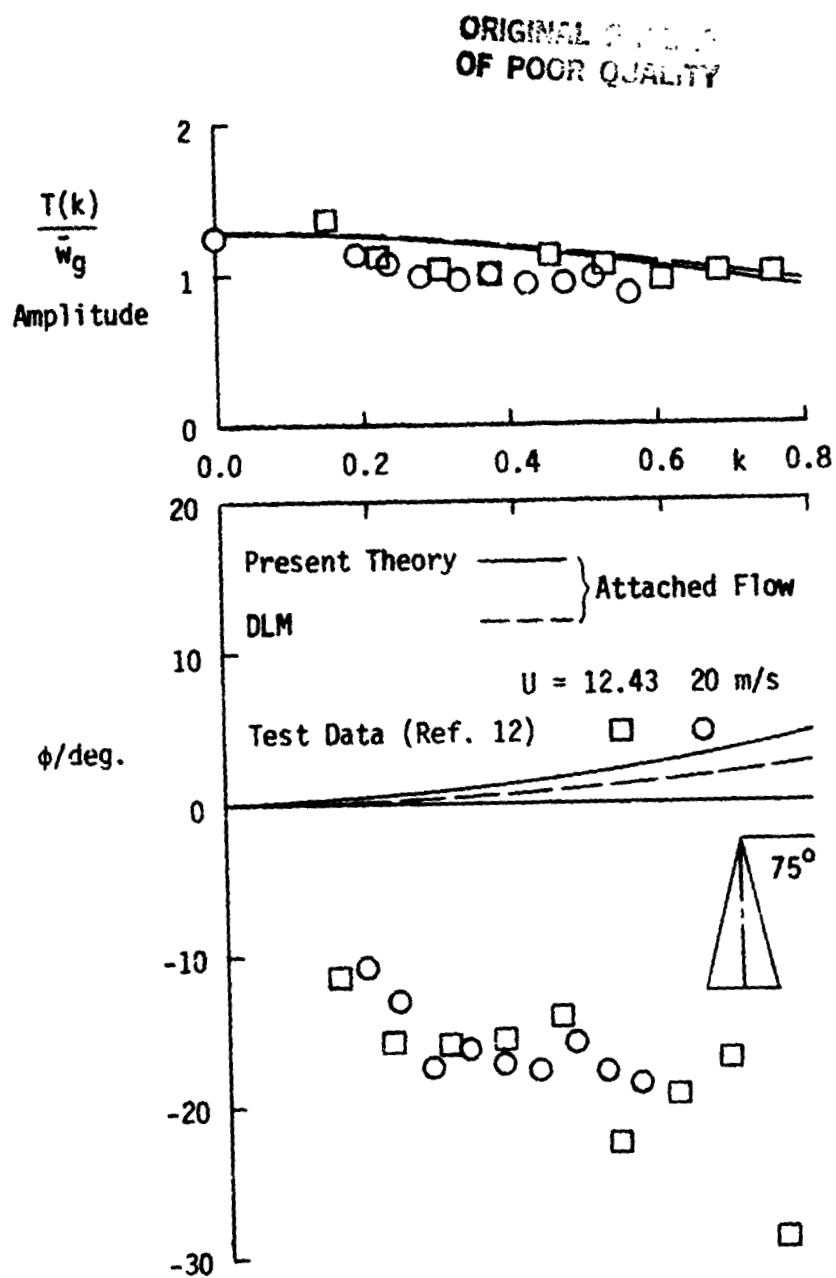


Fig. 6 Incremental lift for a delta wing of $AR = 1$ in sinusoidal gusts for $\alpha = 0^\circ$ with $\bar{w}_g = 0.0314$ and reference point at root 2/3rd chord point.

ORIGINAL PAGE IS
OF POOR QUALITY

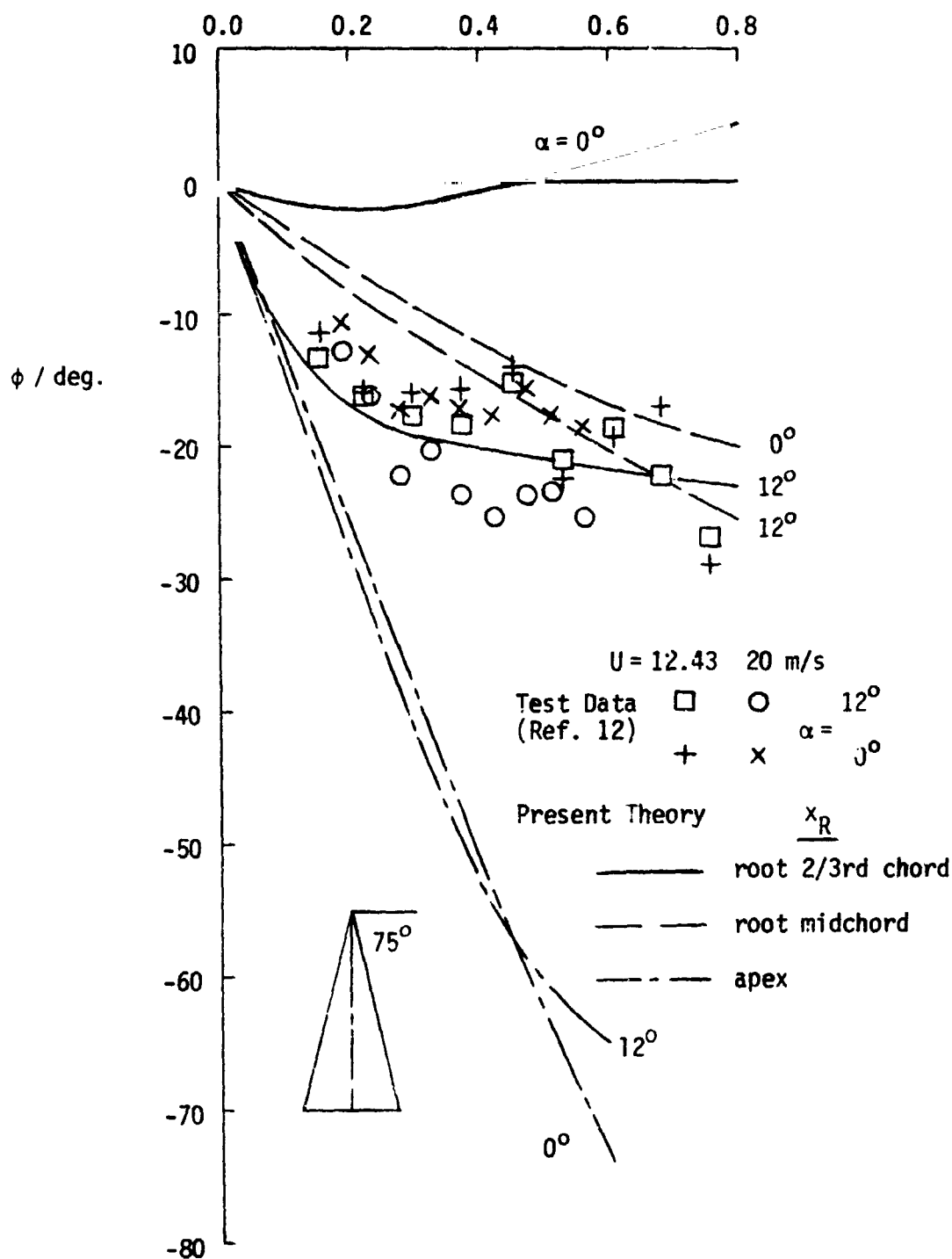


Fig. 7 Variations of phase angle due to changes of angle of attack and reference points for a delta wing of $AR = 1$ in sinusoidal gusts.

ORIGINAL PAGE IS
OF POOR QUALITY

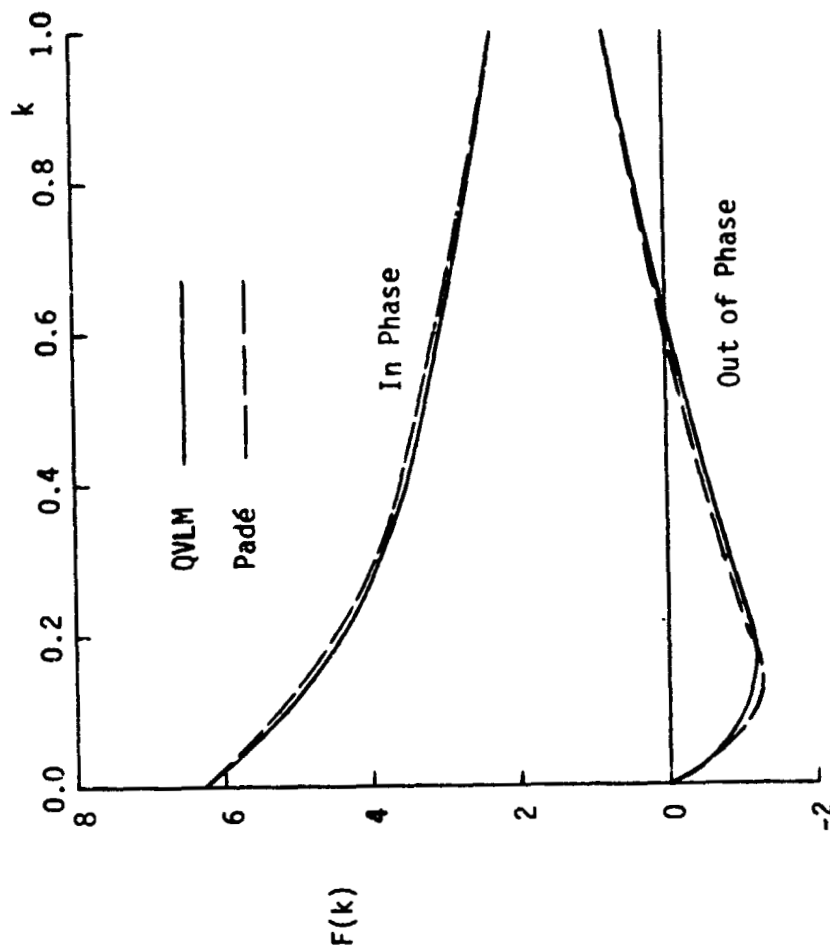


Fig. 8 Oscillatory lift for a thin airfoil due to harmonic gusts with $\bar{w}_g = 1$ at $M = 0$.

ORIGINAL PAGE IS
OF POOR QUALITY

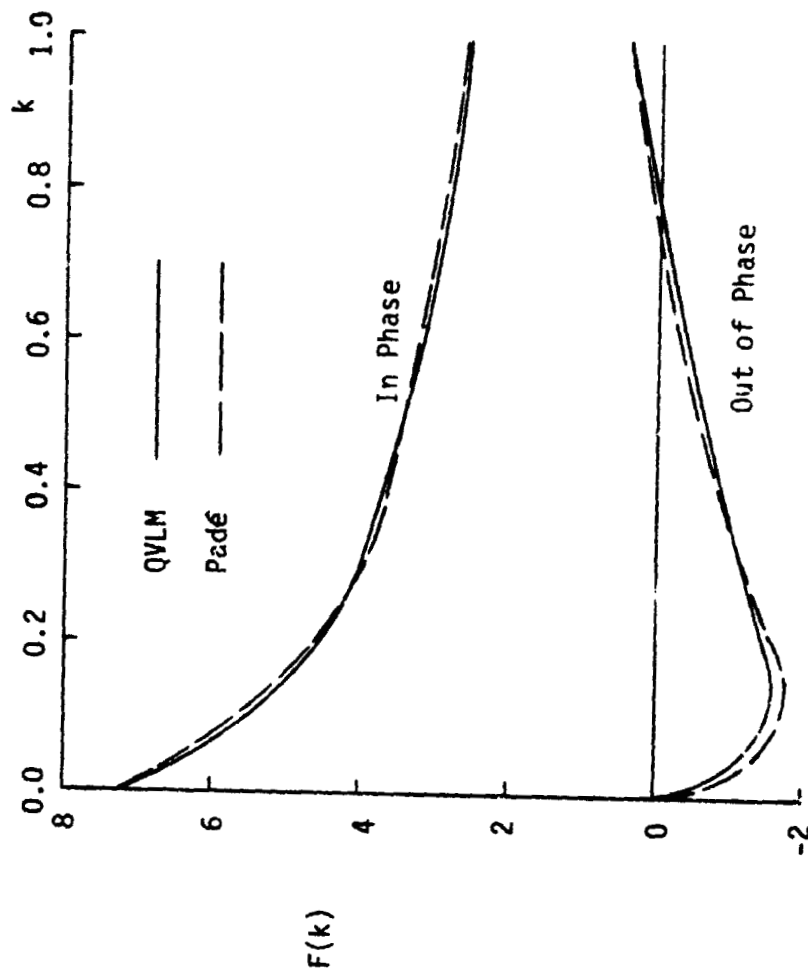


Fig. 9 Oscillatory lift for a thin airfoil due to harmonic gusts with $\bar{w}_g = 1$ at $M = 0.5$.

ORIGINAL FILED IN
OF POOR QUALITY

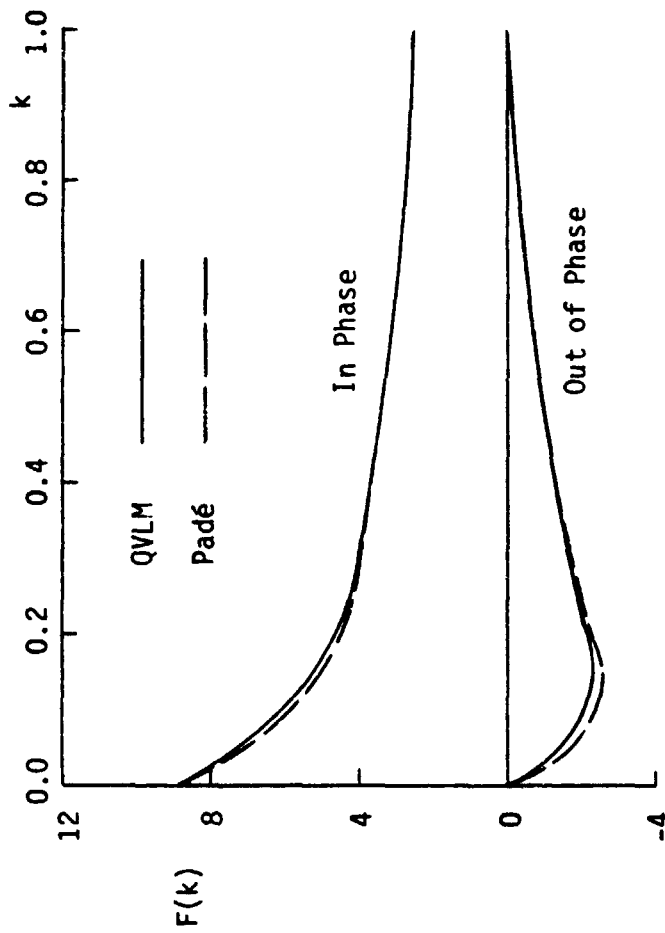


Fig. 10 Oscillatory lift for a thin airfoil due to harmonic gusts with $\bar{w}_g = 1$ at $M = 0.7$.

ORIGINAL PAGE IS
OF POOR QUALITY

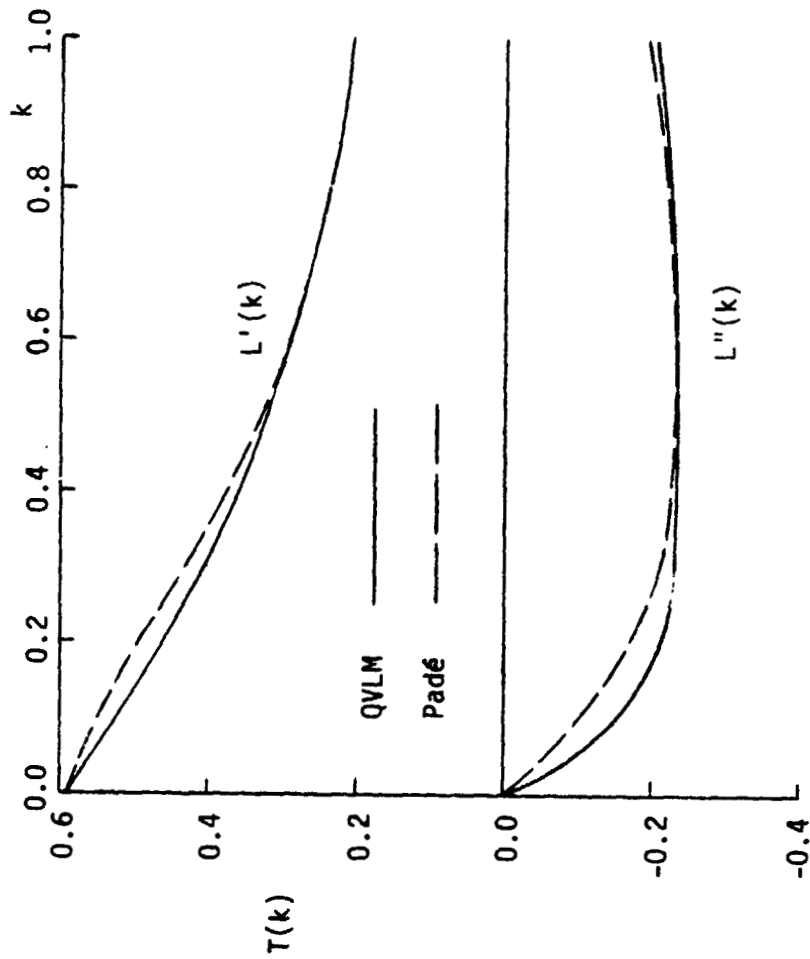


Fig. 11 Oscillatory lift for a delta wing of $AR = 1.2$ in
sinusoidal gusts for $\alpha = 0^\circ$ with $\bar{w}_g = 0.261$ at $M = 0.16$.

ORIGINAL DOCUMENT
OF POOR QUALITY

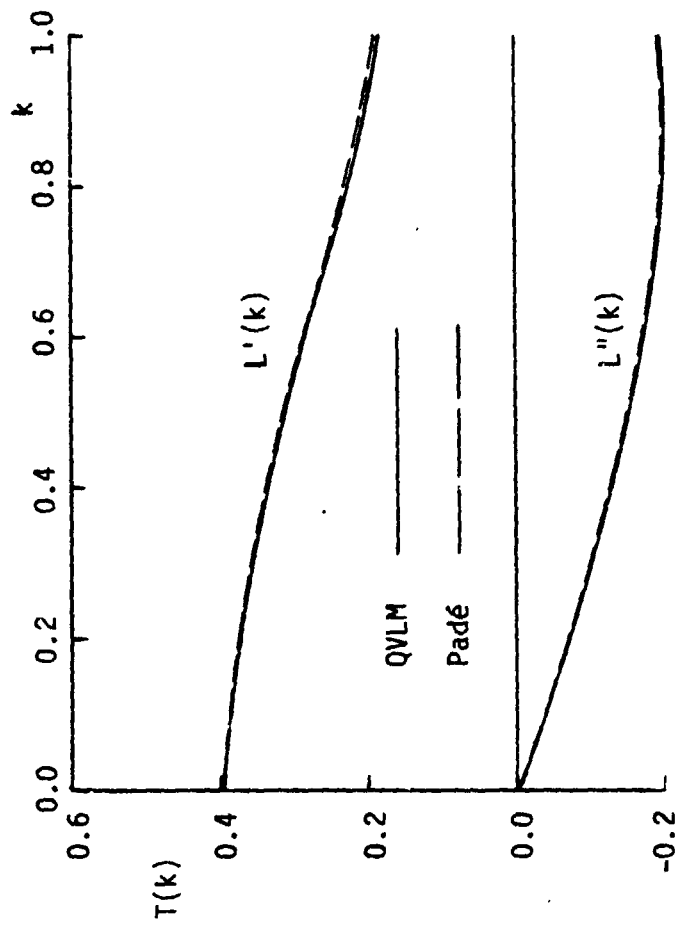


Fig. 12 Oscillatory lift for a delta wing of $AR = 1.2$ in sinusoidal gusts for $\alpha = 14.6^\circ$ with $\bar{w}_g = -0.261$ at $M = 0.16$.

ORIGINAL FILED
OF POOR QUALITY

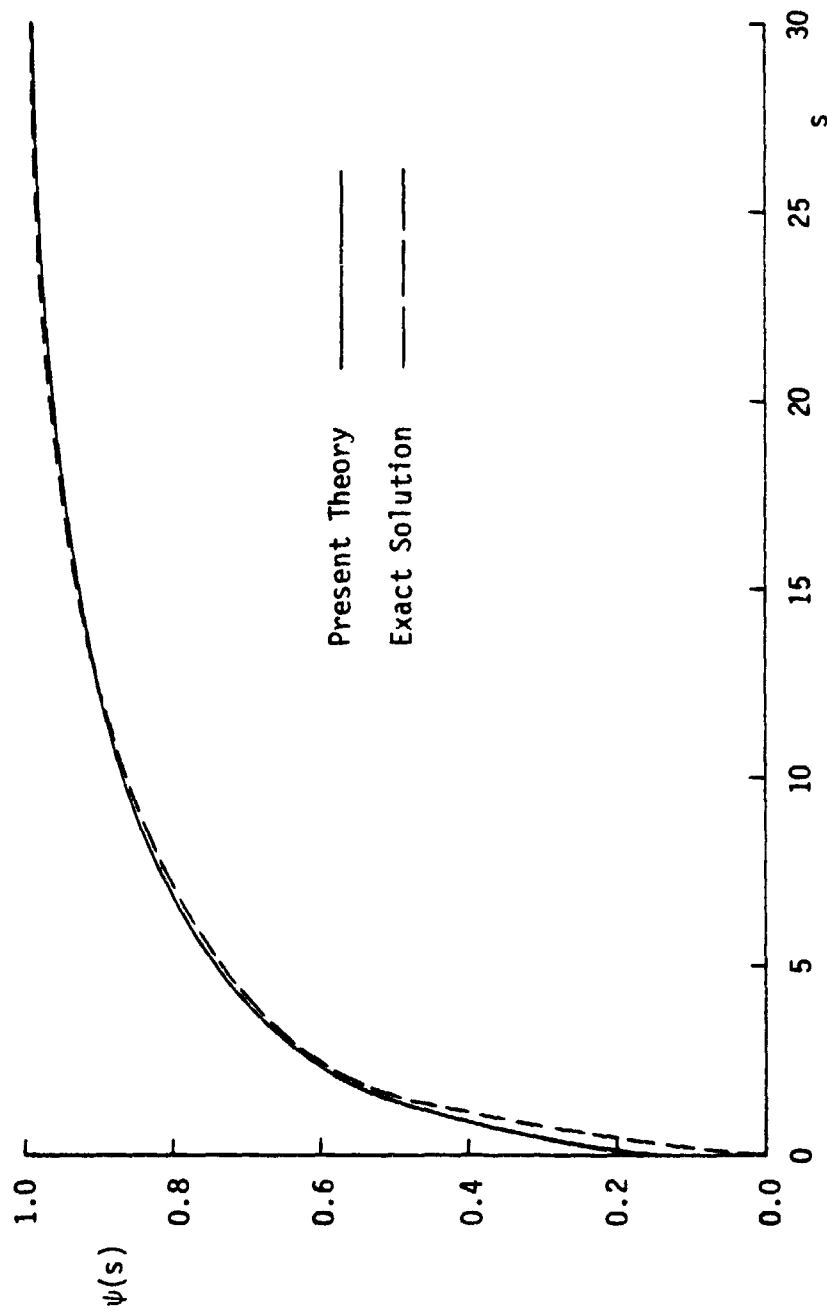


Fig. 13 Indicial lift function from a sharp-edged gust of a thin airfoil at $M=0$.

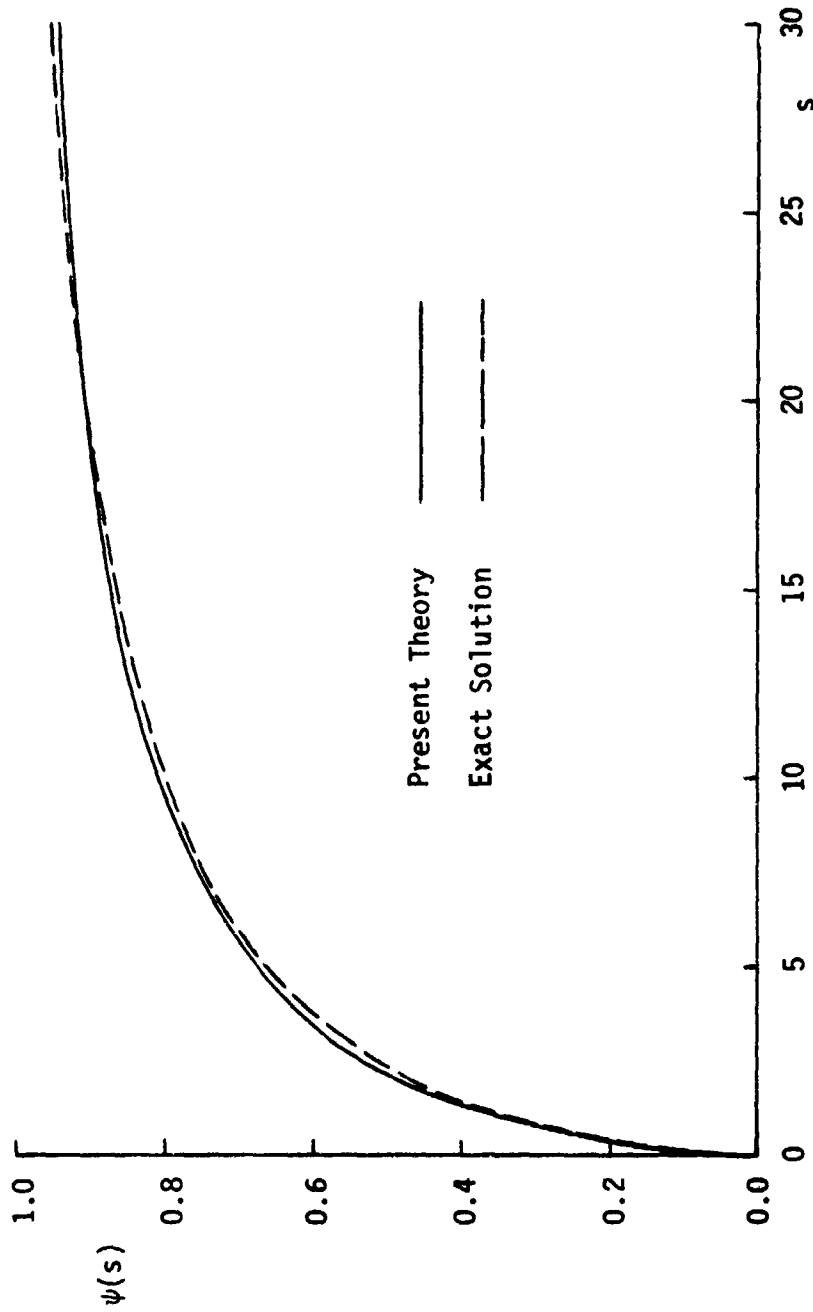


Fig. 14 Indicial lift function from a sharp-edged gust of a thin airfoil at $M=0.5$.

ORIGINAL PAGE IS
OF POOR QUALITY

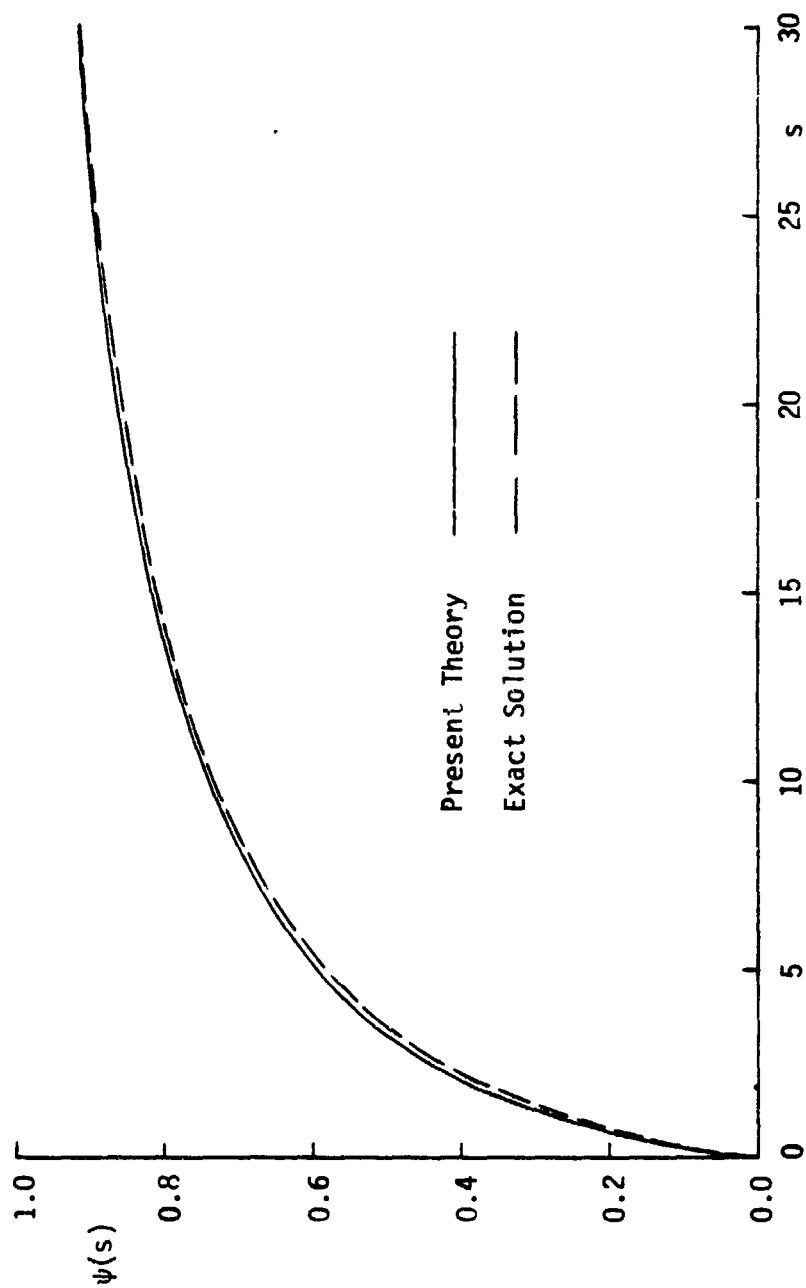
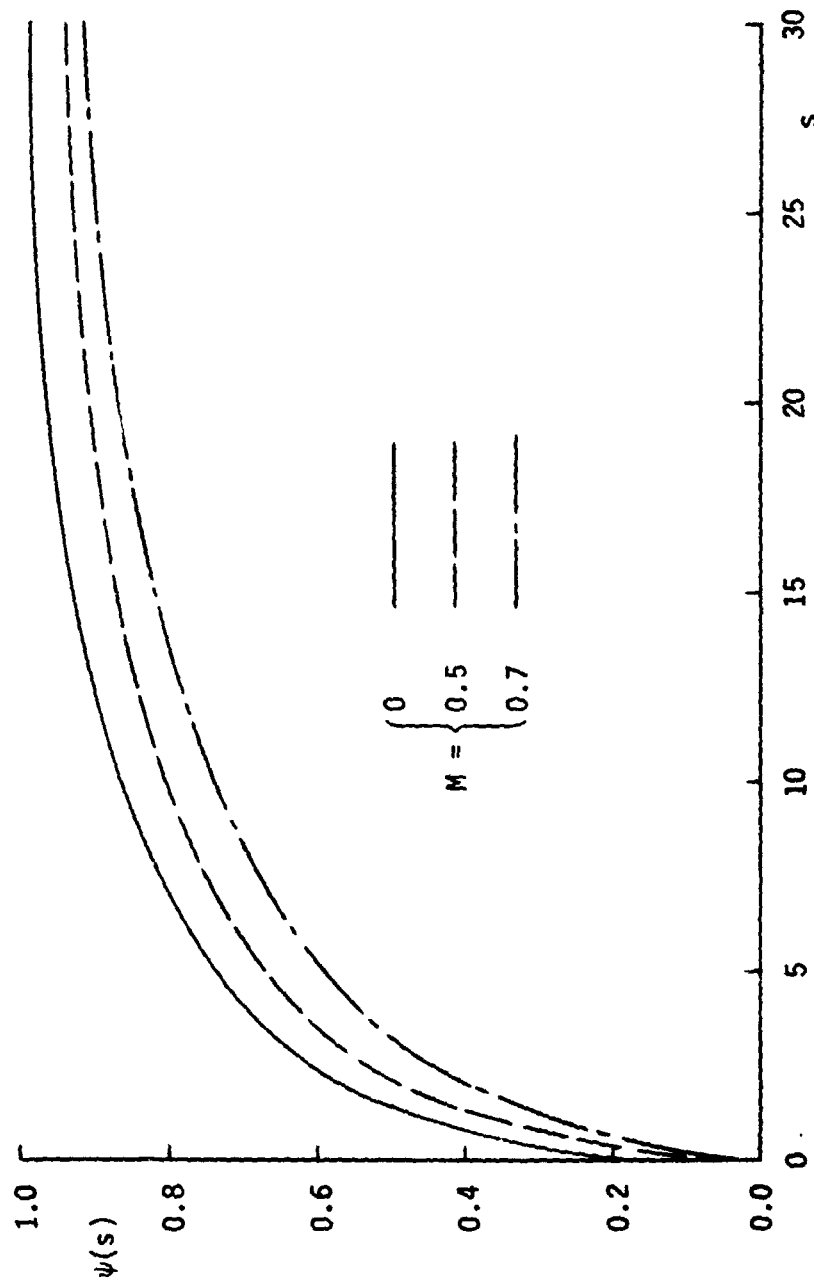


Fig. 15 Indicial lift function from a sharp-edged gust of a thin airfoil at $M=0.7$.



ORIGINAL PAGE IS
OF POOR QUALITY

Fig. 16 Indicial lift function for a thin airfoil entering into a sharp-edged gust in subsonic compressible flow.

ORIGINAL PAGE IS
OF POOR QUALITY

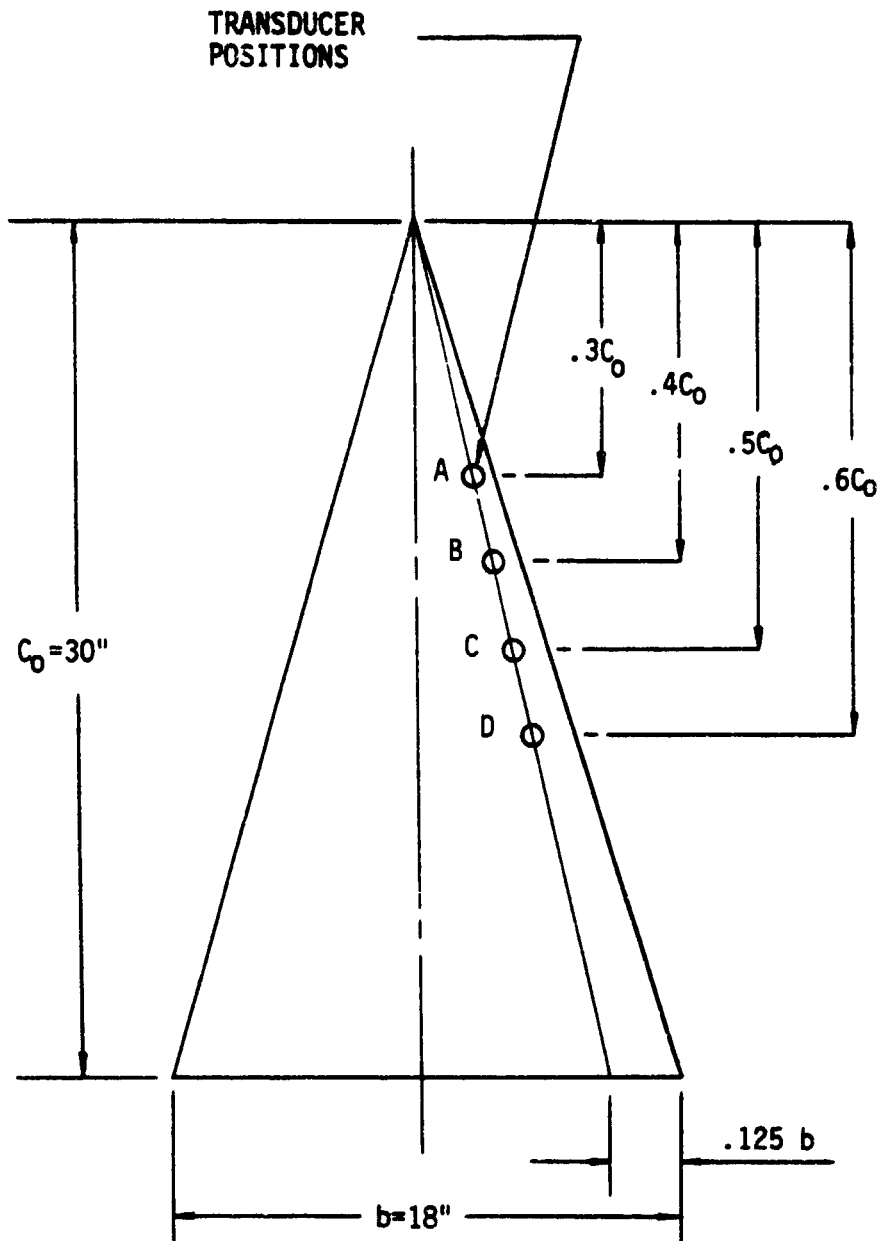


Fig. 17(a) General configuration and transducer positions of the test model in reference 11.

ORIGINAL PAGE IS
OF POOR QUALITY

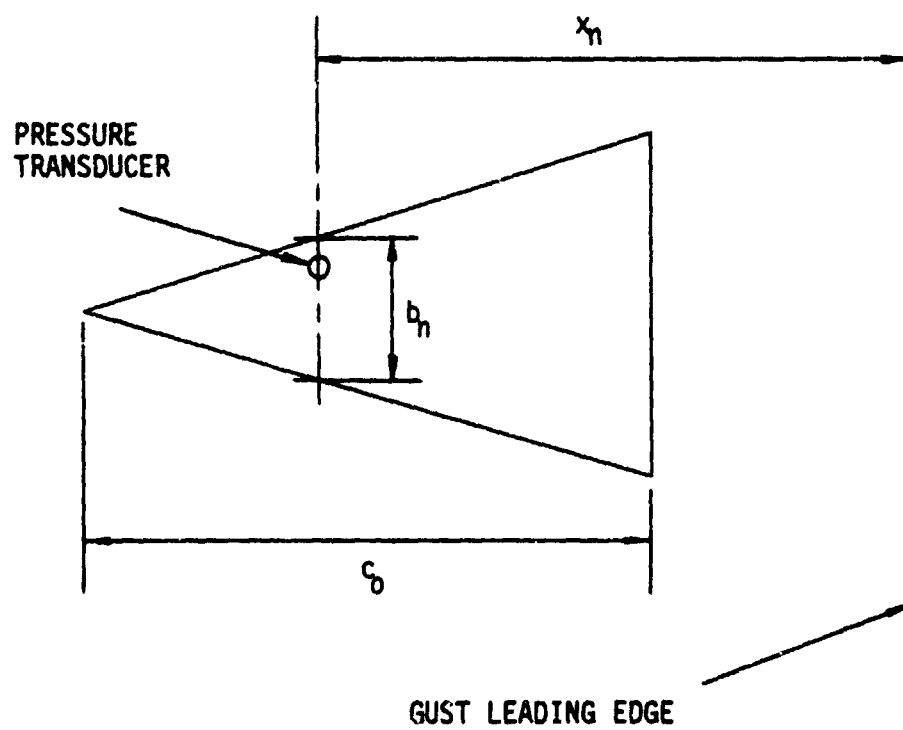


Fig. 17(b) Definitions of the local span and distance parameter penetrated into the vertical gusts.

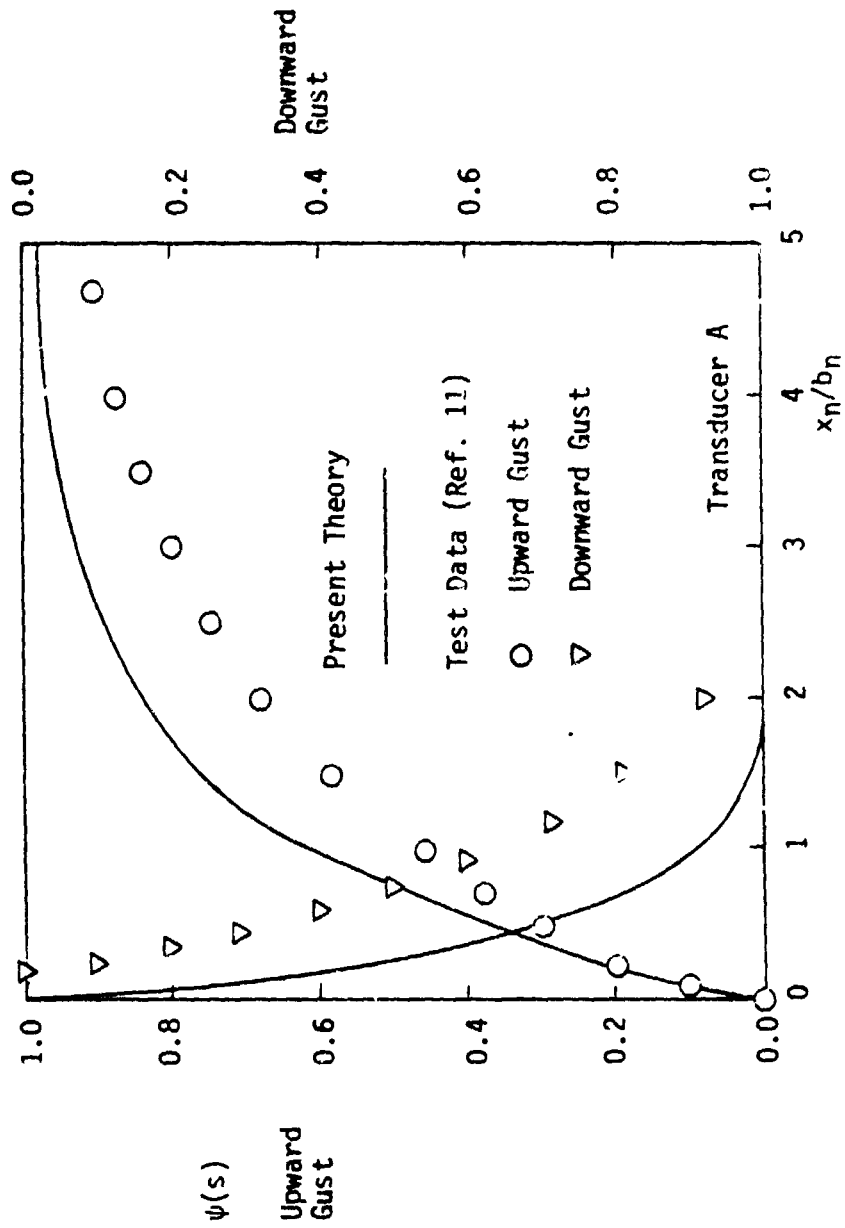


Fig. 18 Trend of indicial lift function from vertical gusts of a delta wing of $AR = 1.2$ at $M = 0.16$.

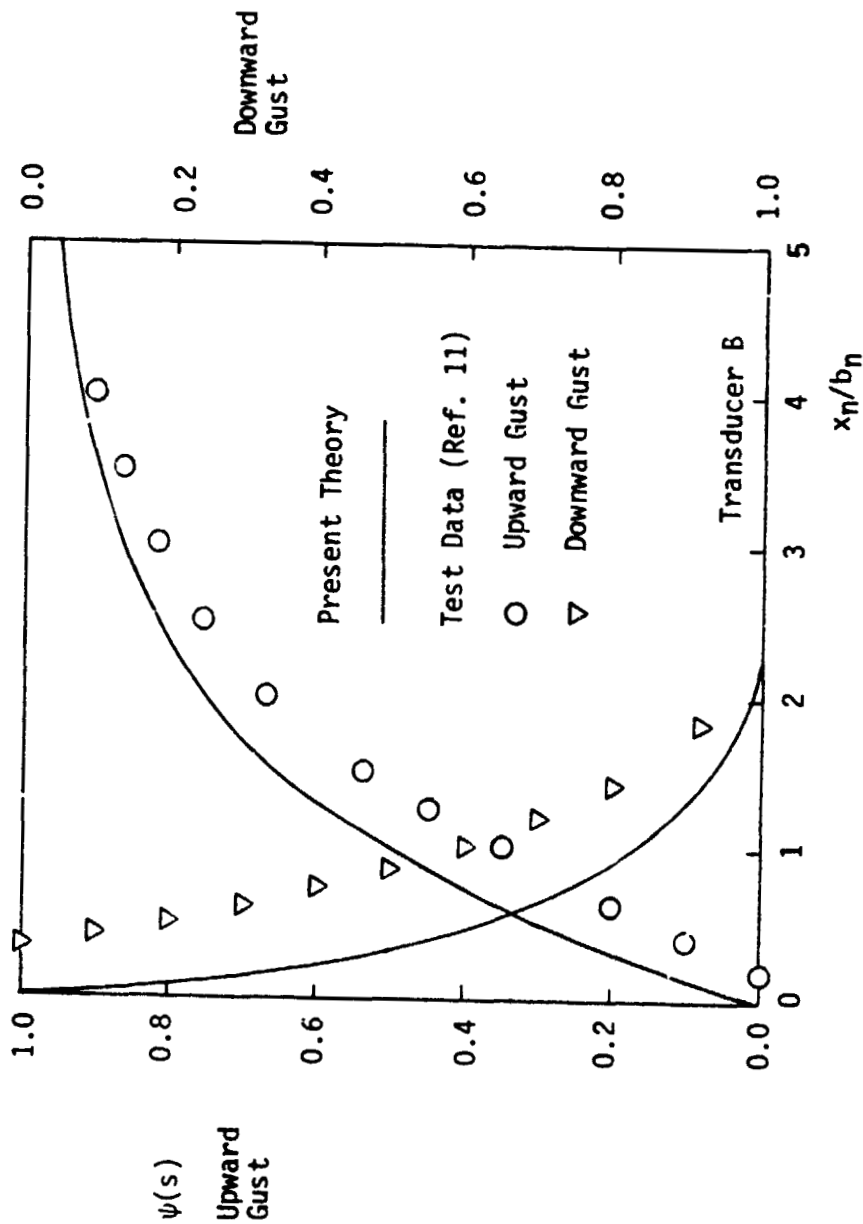


Fig. 18 Continued.

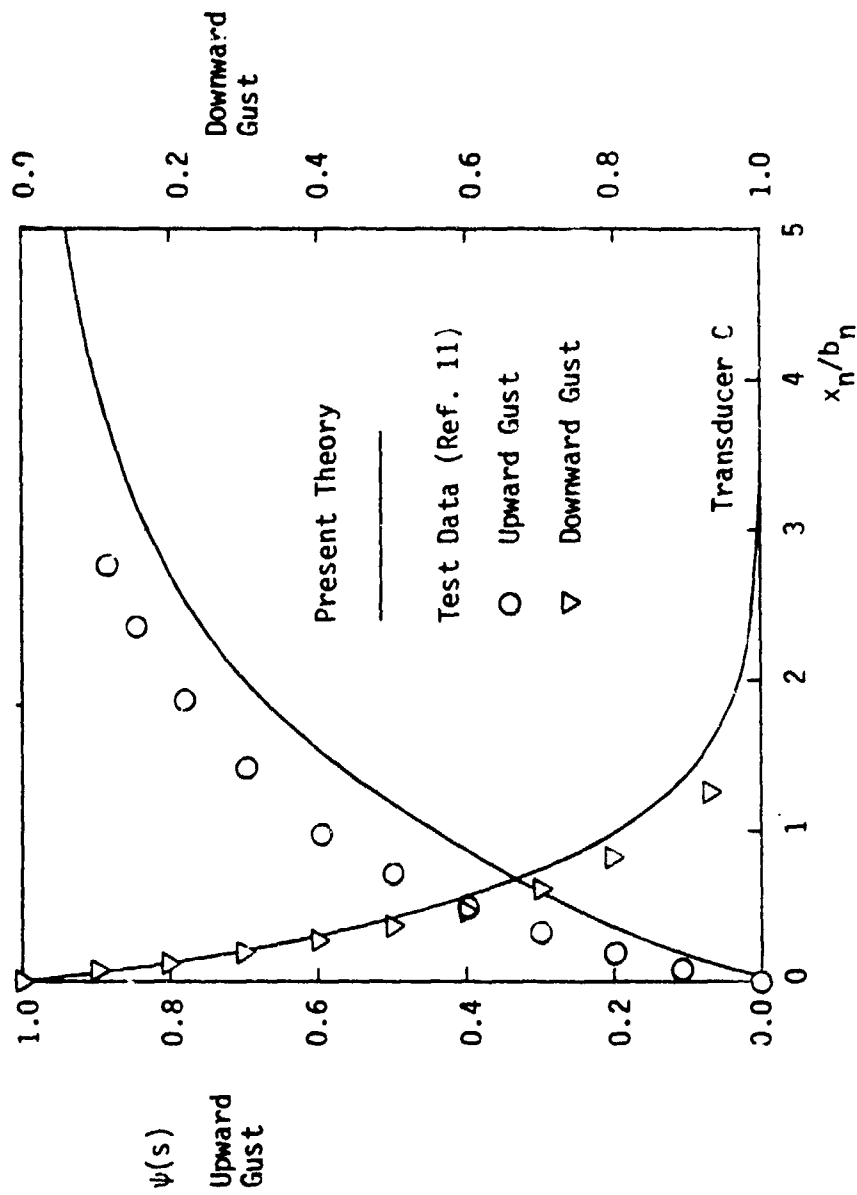


Fig. 18 Continued.

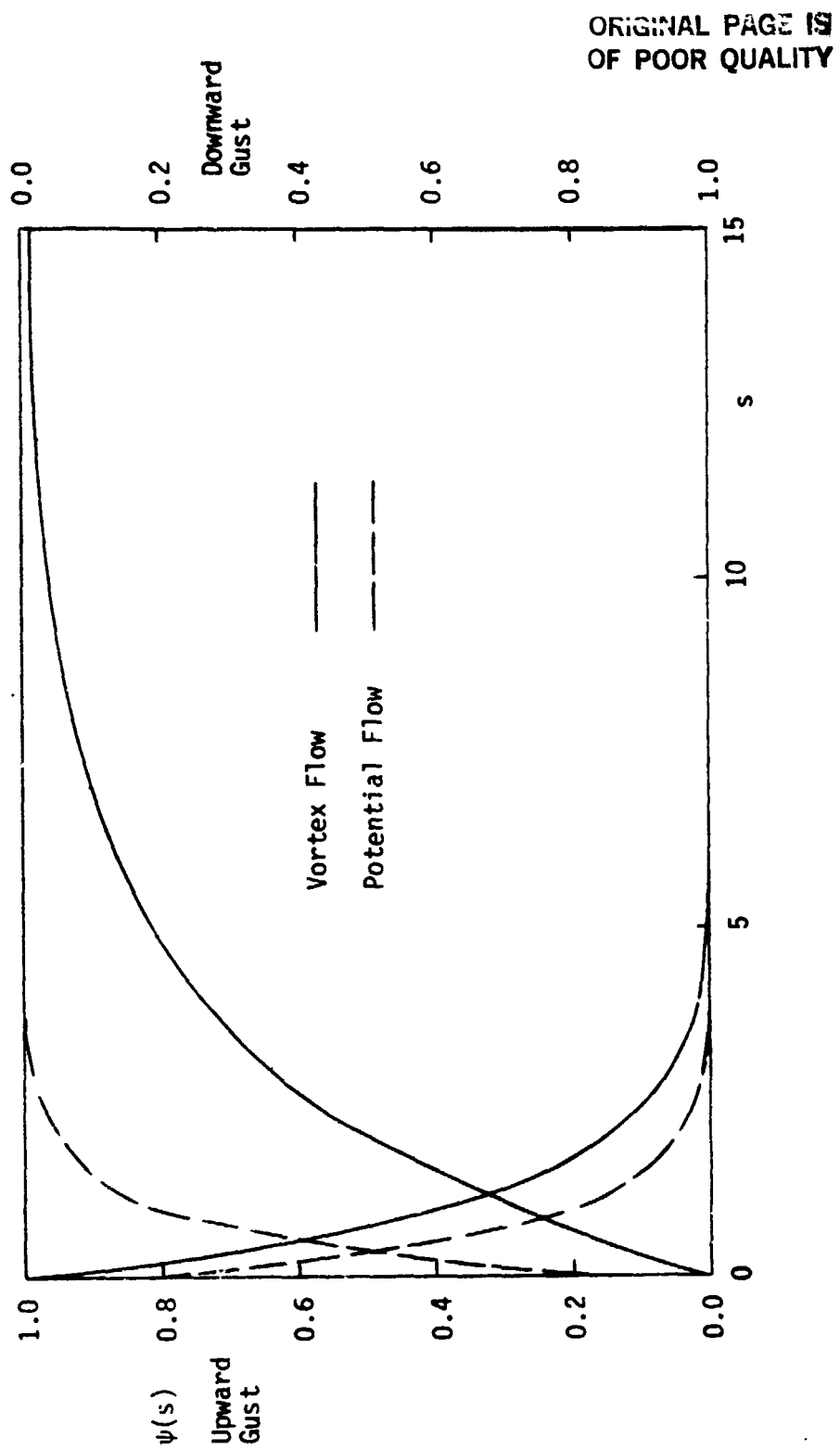


Fig. 19 Indicial lift function for a delta wing of $AR = 1.2$ entering into vertical gusts at $M = 0.16$.

ORIGINAL PAGE IS
OF POOR QUALITY

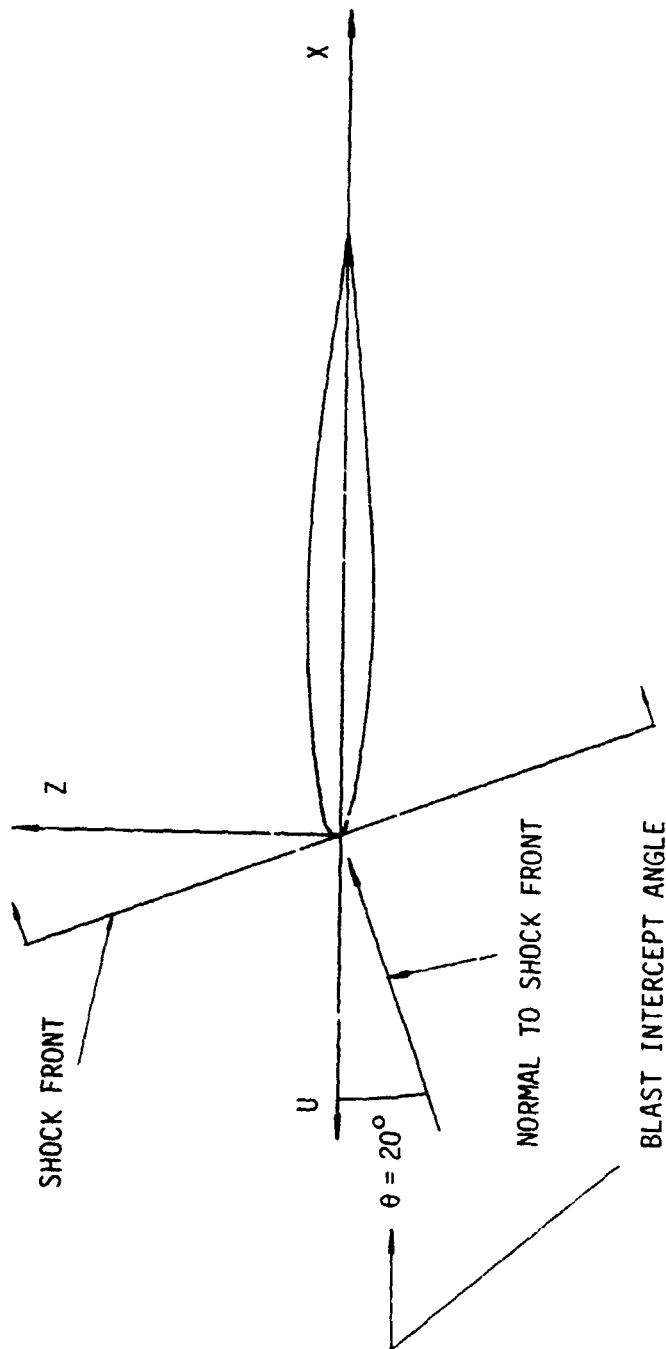
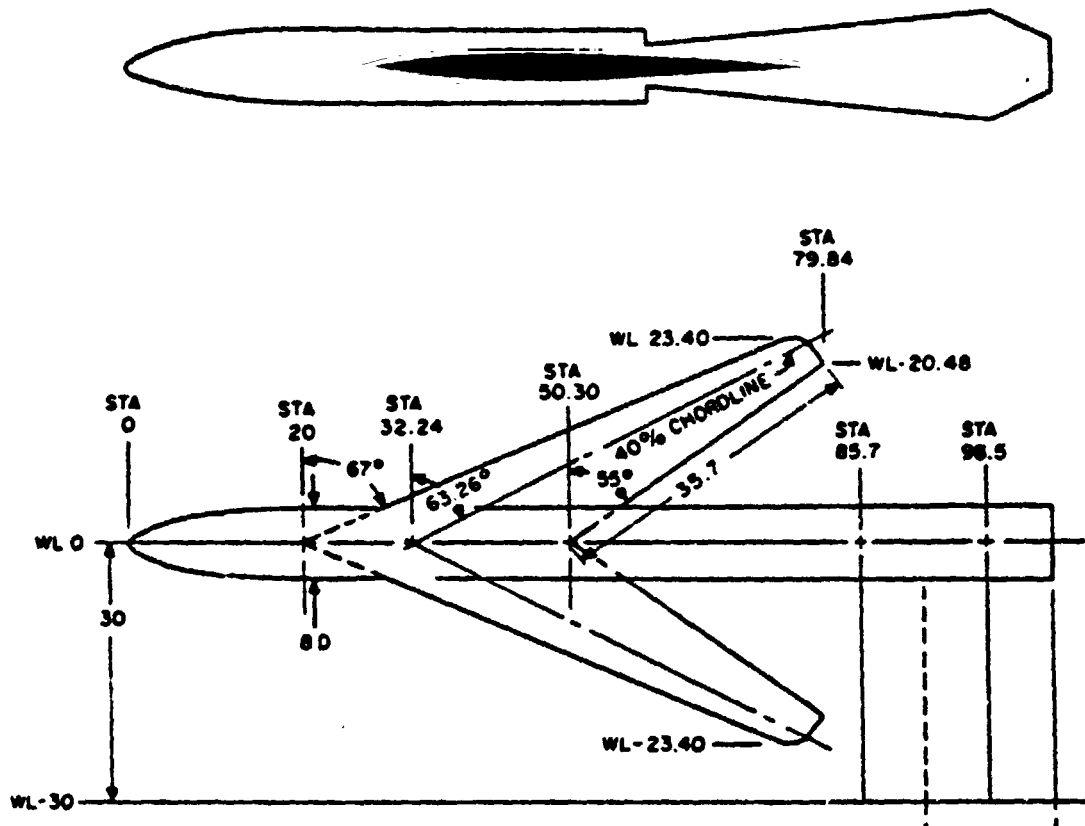


Fig. 20 Thin wing intercepted by a blast wave moving with sonic speed.

ORIGINAL PAGE IS
OF POOR QUALITY



| | | | |
|---------------------------------|----------|---|----------------------|
| Wing Span | 46.80 in | Fuselage Diameter | 8 in |
| Wing Aspect Ratio | 2.47 | Wing Section | 64A012 |
| Taper Ratio | 0.29 | Thickness Ratio | 12% |
| Centerline Chord (At W.L.=0) | 30.60 in | (In Streamwise Sections) | |
| Leading Edge Sweep | 67.0 deg | Mean Chord | 18.95 in |
| Quarter-Chord Sweep | 64.8 deg | Wing Planform Area | 6.16 ft ² |
| Trailing Edge Sweep | 55.0 deg | (Including Portion Submerged Within Fuselage) | |

Fig. 21 General configuration of the test model used for nuclear blast response (taken from reference 17).

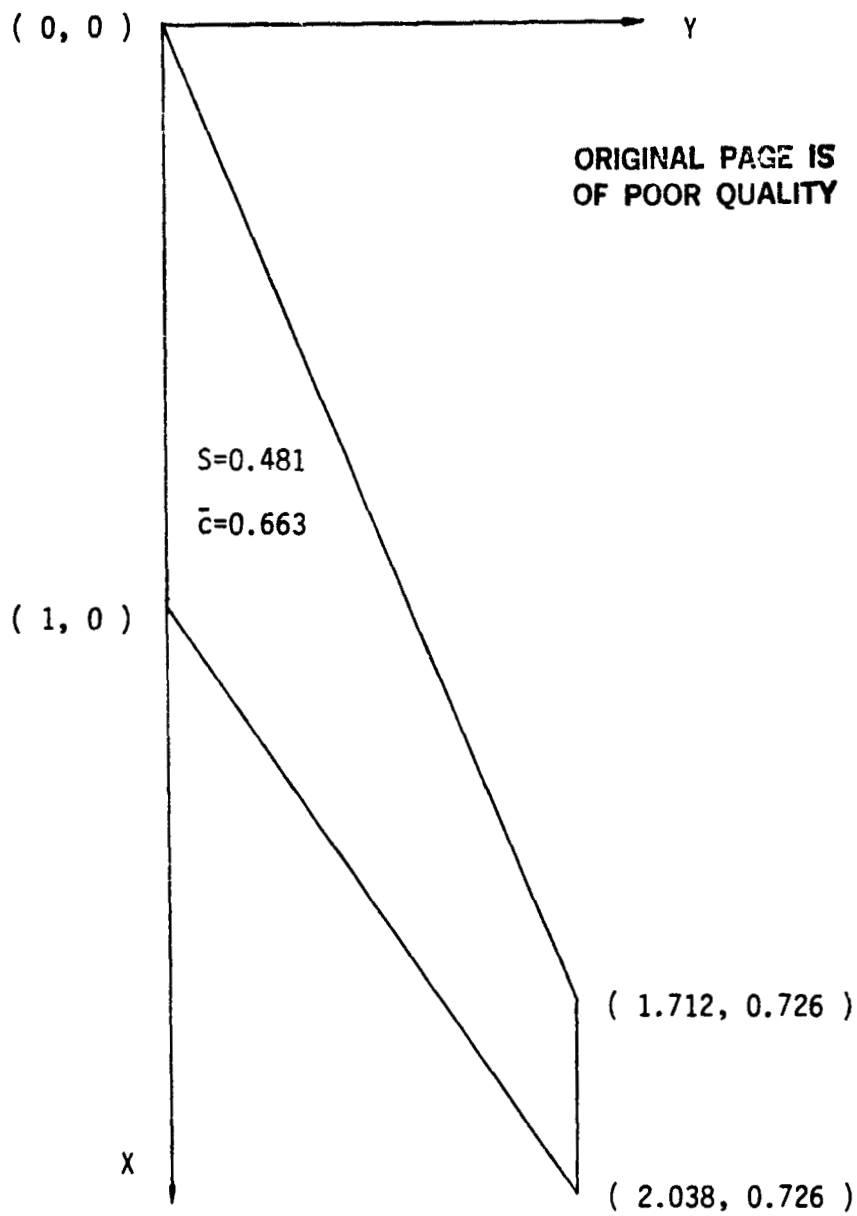


Fig. 22 Simplified wing planform used by the present theory for nuclear blast response analysis.

STATION 50/25 TRANSducer 13

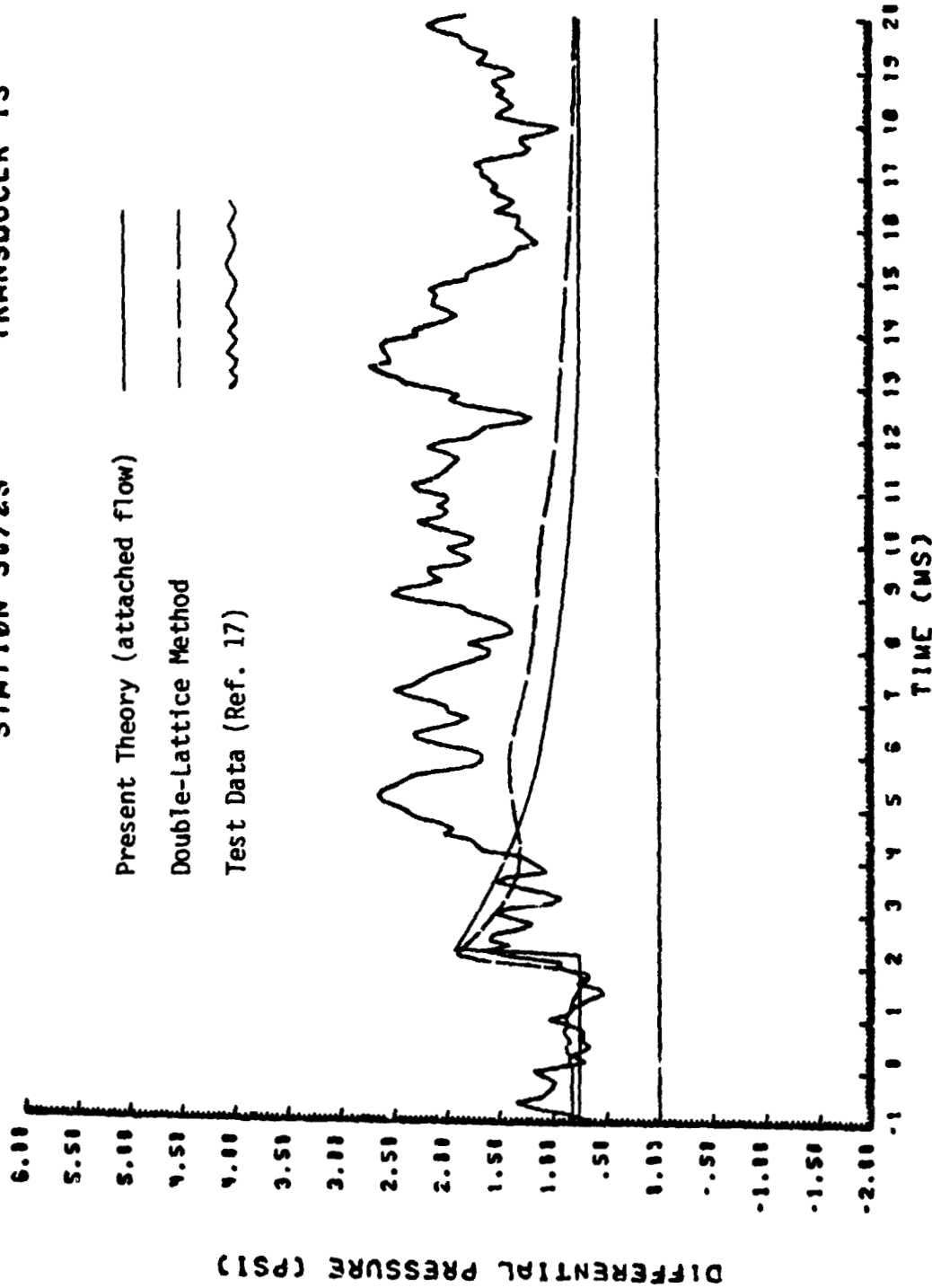


Fig. 23 Pressure variation of the test wing due to nuclear blast waves with $\theta = 20^\circ$ for $\alpha = 3.2^\circ$ at $M = 0.76$ (reproduced from reference 17).

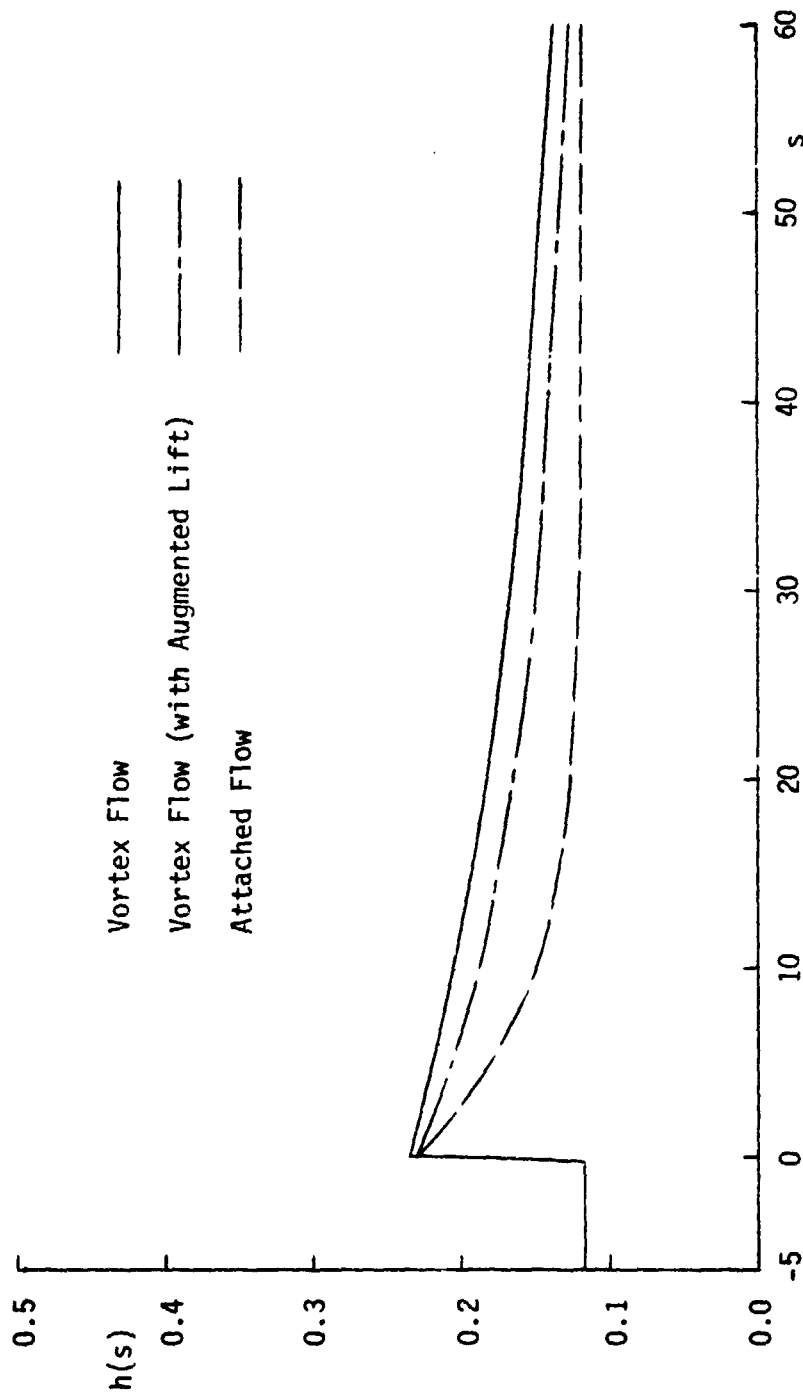


Fig. 24 Impulse lift function of the test wing due to nuclear blast waves with $\theta = 20^\circ$ for $\alpha = 3.2^\circ$ at $M = 0.76$.

ORIGINAL PAGE IS
OF POOR QUALITY

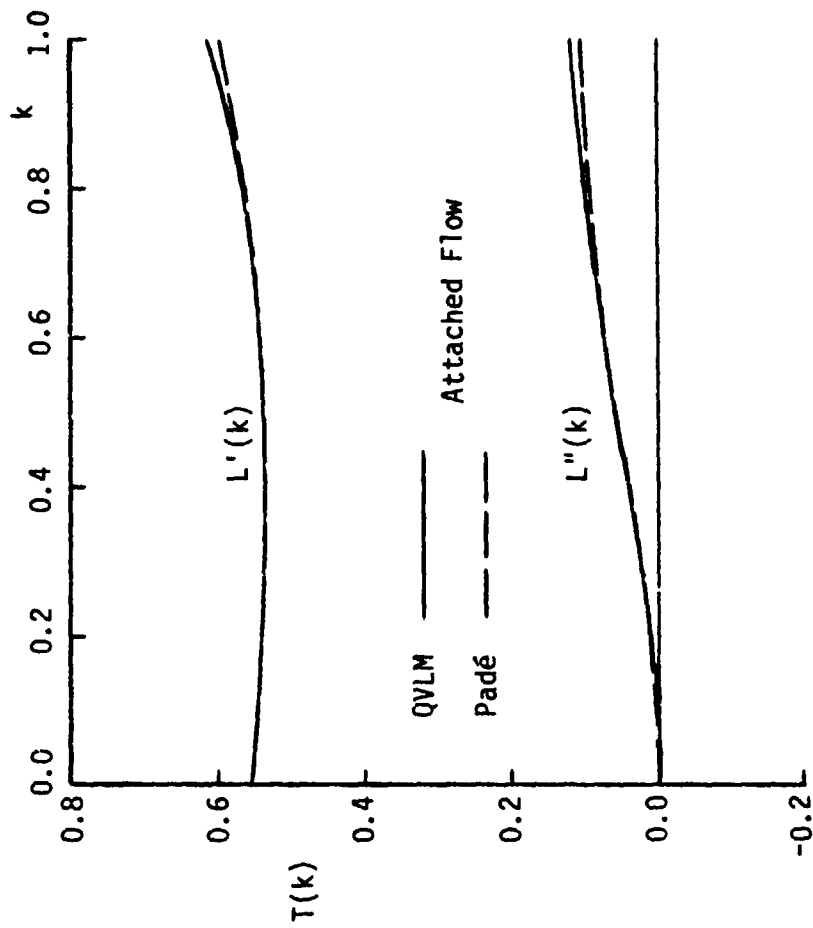


Fig. 25 Oscillatory lift for a delta wing of $R=2$ due to a blast wave for $\alpha = 15^\circ$ with $\bar{w}_g = 0.268$ at $M = 0.5$.

ORIGINAL PAGE IS
OF POOR QUALITY

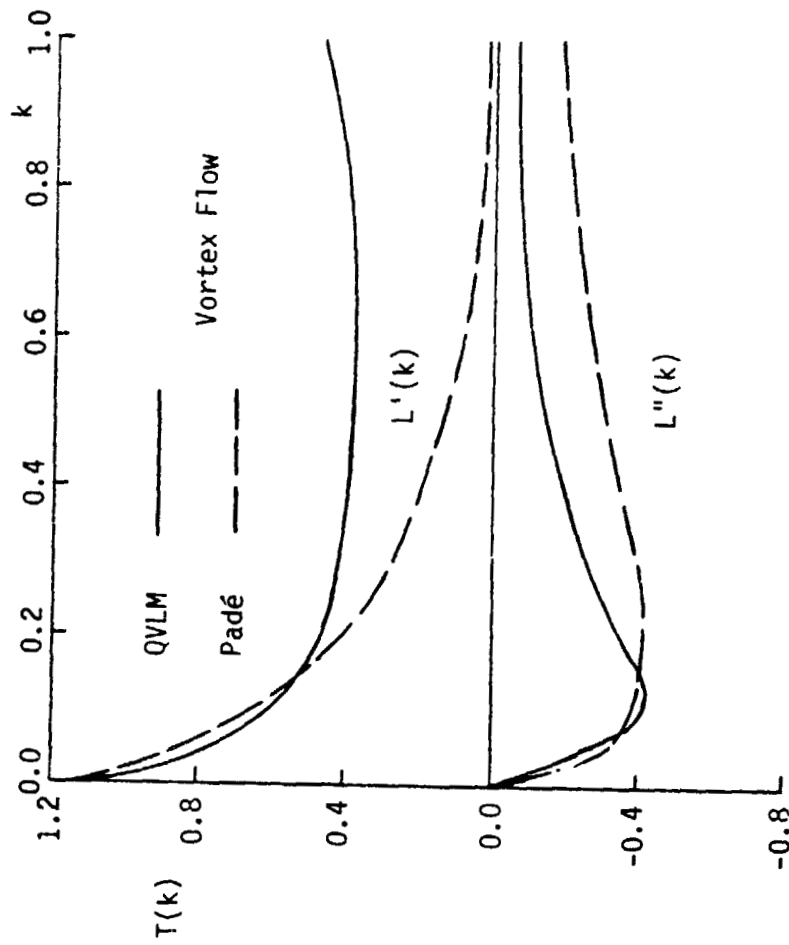


Fig. 26 Oscillatory lift for a delta wing of $R=2$ due to a nuclear blast wave for $\alpha = 15^\circ$ with $\bar{w}_g = 0.268$ at $M = 0.5$.